UNIVERSITA' DEGLI STUDI DI NAPOLI "FEDERICO II"

FACOLTA' DI MEDICINA E CHIRURGIA

Dottorato di ricerca in
MORFOLOGIA CLINICA E PATOLOGIA
Dipartimento di Scienze Biomorfologiche e Funzionali

Formation of Temporary Niches Is Required for Bone Marrow Cells To Adopt the Cardiomyogenic Fate *In Vivo*

Relatore

Prof. S. Montagnani

Correlatore

Prof . Piero Anversa

Candidata

Serena Vitale

Tesi svolta presso il Cardiovascular Research Institute,

New York Medical College,Valhalla ,NY

Formation of Temporary Niches Is Required

for Bone Marrow Cells

To Adopt the Cardiomyogenic Fate *In Vivo*

So far so close.

Summary

The possibility that adult bone marrow cells retain a remarkable degree of developmental plasticity and acquire the cardiomyocyte lineage after infarction has been challenged and the notion of bone marrow cell transdifferentiation has been questioned. The center of the controversy is the lack of unequivocal evidence in favor of myocardial regeneration by the injection of bone marrow cells in the infarcted heart. Because of the great interest in cell-based therapy for heart failure, several approaches including gene reporter assay, genetic tagging, cell genotyping, PCR-based detection of donor genes, and direct immunofluorescence with quantum dots were employed to document or disprove bone marrow cell transdifferentiation into functionally competent myocardium. Together, our studies indicate that locally delivered bone marrow cells generate *de novo* myocardium composed of integrated cardiomyocytes and coronary vessels. Importantly, this process occurs independently of cell fusion and ameliorates structurally and functionally the outcome of the post-infarcted heart.

Introduction

Endothelial progenitor cells, mononuclear bone marrow cells, and CD34 positive cells have been administered to patients affected by acute myocardial infarction or chronic ischemic heart failure. These interventions have had positive outcome documenting not only the feasibility and safety of this therapeutic approach but also beneficial effects on cardiac function. While patients are currently enrolled in large clinical trials, the mechanisms by which bone marrow progenitor cells (BMPCs) ameliorate the function of the infarcted heart is currently under intense debate. Additionally, the documentation of cardiac specific adult progenitor cells (CPCs) has created great expectation concerning the utilization of this new cell for the management of the human disease. Theoretically, the most logic and potentially powerful cell to be employed for cardiac repair is the CPC. It is intuitively apparent that if the adult heart possesses a pool of primitive, undifferentiated, multipotent cells, these cells must be tested first, before more complex and unknown cells are explored. The attraction of this approach is its simplicity. Cardiac regeneration would be accomplished by enhancing the normal turnover of myocardial cells. However, difficulties exist in the acquisition of myocardial samples in humans, and in the isolation and expansion of CPCs in quantities that can be employed therapeutically. Conversely, bone marrow progenitor cells (BMPCs) constitute an appealing form of cell intervention; BMPCs can be easily collected from bone marrow aspirates or the peripheral blood upon their mobilization from the bone marrow with cytokines. At present, it is unknown whether CPCs and BMPCs are similarly effective in reconstituting

dead myocardium after infarction or limitations exist in CPC growth and BMPC transdifferentiation resulting in inadequate restoration of lost tissue. Also, BMPCs may constitute a necessary initial form of intervention for the infarcted heart whereas CPCs might be employed later during the chronic evolution of the cardiac myopathy. Thus, a fundamental question to be addressed is whether BMPCs are capable of promoting myocardial regeneration with the formation of functionally competent myocytes and coronary vessels in models of ischemic heart failure**.**

Cardiac repair after infarction is mediated by several factors including (**a**) number of cells to be administered, (**b**) cell death and survival in the hostile milieu of the infarct and peri-infarcted region, (**c**) cell engraftment, and (**d**) cell growth and differentiation. An additional critical variable of BMPCs is their level of plasticity, which is dictated by their ability to acquire the myocyte, and vascular smooth muscle (SMC) and endothelial cell (EC) lineages. Moreover, the injected BMPCs can contribute indirectly to cardiac regeneration by releasing a variety of peptides that exert a paracrine action on the myocardium and its resident progenitor cells. These mechanisms are not mutually exclusive and both progenitor cell populations may participate directly and indirectly in the repair process. In all cases, progenitor cells have to engage themselves in homing into the myocardium to perform specific functions. **These biological processes depend on a successful interaction between BMPCs and tissue microenvironment**.

Importantly, the unfavorable microenvironment of the infarct varies with time and infarct healing. Apoptotic myocytes and vascular cells are replaced by diffuse cell necrosis, inflammation, and myocardial scarring. These evolving characteristics of the

dead myocardium may have consequences on BMPC homing, survival, growth and differentiation.

Preliminary published observations indicate that the stem cell antigen c-kit is expressed in a population of BMPCs that are capable of differentiating into cardiomyocytes, SMCs and ECs restoring in part large myocardial infarcts and ventricular performance. Therefore, the stem cell epitope c-kit was employed to isolate progenitor cells from the bone marrow and the cells were injected locally within the myocardium bordering the infarct. Although this approach allowed us to obtain a reasonably homogeneous preparation of progenitor cells, it has limitations related to the uncommitted or early committed state of the cells, their quiescent or cycling condition, and their migratory properties. However, the collection of progenitor cell classes by stem cell antigens remains the most reasonable and sensitive strategy to date.

The mechanisms that guide stem cell homing in the myocardium are not completely understood. Cardiac injury may be necessary for migration and long-term engraftment of stem cells in the myocardium. In the absence of tissue damage, the implanted stem cells are at growth disadvantage with respect to the endogenous stem cells. The ischemic myocardium provides a microenvironment that is particularly rich in cytokines favoring seeding, survival and growth of progenitor cells. The binding of SDF-1 to its receptor CXCR4 is critical in promoting homing of BMPCs to the bone marrow and distant organs, although IGF-1 and HGF may be crucial in opposing death signals and facilitating migration, respectively. SDF-1, IGF-1, and HGF are upregulated in the border zone acutely after infarction and may enhance BMPC viability, translocation and homing. Engraftment of BMPCs necessitates the formation of adherens and gap junctions

with resident myocytes and fibroblasts, which are the supporting cells in the niches and anchor the injected cells to the host myocardium. Interaction between integrin receptors on progenitor cells and extracellular matrix proteins is fundamental for cell lodging, division, and maturation. BMPCs colonize the heart and might possess a high degree of plasticity adapting rapidly their phenotype to the cardiac microenvironment. The process of transdifferentiation may alter the growth behavior of BMPCs, which may lose in part their ability to divide after the acquisition of the myocyte phenotype. Similarly, myocytes derived from BMPCs may possess inherent limitations in the acquisition of the adult phenotype. However, the opposite may also be true and BMPCs may retain even after transdifferentiation a strong regenerative capacity representing an appropriate cell for the damaged heart. Thus, **the growth properties of BMPCs and derived myocytes were established to resolve this biologically and clinically relevant issue**.

Bone Marrow Cells and Cardiac Repair

To date, the hematopoietic stem cell appears to be the most versatile stem cell in crossing lineage boundaries and the most prone to break the law of tissue fidelity[1,2]. Early studies on bone marrow cell (BMC) differentiation into myocardium have generated great enthusiasm[3-5] but other observations have rejected the initial positive results[6-8] and promoted a wave of skepticism about the therapeutic potential of BMCs for the injured heart[9]. The major criticisms include inaccurate interpretation of the original data due to autofluorescence artifacts and the lack of genetic markers for the recognition of the donor BMCs and their progeny[6-9]. In fact, the apparent improvement in function of the infarcted heart observed following BMC administration was assumed to be mediated by unidentified paracrine effects exerted by the delivered cells on the surviving myocardium[10].

In an attempt to address these critical issues, female infarcted mice were injected with male EGFP-positive c-kit-positive BMCs (c-kit-BMCs) and the consequences of this intervention on post-infarction remodeling were determined 5, 10 and 30 days later. Additionally, another set of experiments was conducted in which donor c-kit-BMCs were obtained from male mice carrying EGFP or a c-myc-tagged nuclear Akt transgene under the control of the cardiac specific α-myosin-heavy-chain promoter[11]. Similarly, the efficacy of this protocol on the post-infarcted heart was evaluated 5, 10 and 30 days after treatment. These three models allowed us to determine the destiny of c-kit-BMCs within the recipient heart by genetic tagging with EGFP, cell fate tracking with EGFP and c-

myc, sex-chromosome identification by *in situ* hybridization, EGFP and c-myc gene detection by PCR.

An essential premise of these studies was the development of a methodology in which immunolabeling of proteins was obtained in the absence of the autofluorescence inherent in tissue sections of formalin-fixed myocardium. This objective was achieved by implementing a new technology by which primary antibodies are directly labeled by small semi-conductor particles termed quantum dots[12]. This procedure eliminates the needs for secondary antibody staining and avoids the interference of autofluorescence in the specificity of the reaction. The excitation wavelength of quantum dots is widely separated from the emission wavelength and the spectrum of autofluorescence never coincides with the emission wavelength (**Fig. 1a-d**). Moreover, myocardial components labeled by antibodies conjugated with quantum dots preserve fluorescence intensity and do not experience a time-dependent fluorescence decay commonly encountered with standard fluorochromes such as rhodamine or fluorescein. Quantum dots are resistant to photobleaching and samples can be examined for extended periods by confocal or epifluorescence microscopy without altering the intensity of labeling or the resolution of the labeled structures (**Fig. 1e-h**).

Engraftment of BMCs

Given the question whether BMCs transdifferentiate into the cardiogenic lineage, donor male c-kit-BMCs were obtained from EGFP transgenic mice or from transgenic mice which carried a cardiac specific EGFP or a c-myc-tagged nuclear Akt. The male c-kit-BMCs were then injected acutely after infarction in female wild-type mice. Within 12-36 hours, male c-kit-BMCs engrafted within the viable myocardium bordering the infarct

through the formation of junctional and adhesion complexes with adjacent myocytes and fibroblasts (**Fig. 2a, b**). Myocytes and fibroblasts function as supporting cells within the cardiac stem cell niches[13] and c-kit-BMCs have to form temporary niches within the host myocardium to home, survive and grow in this unfamiliar environment[14]. By this mechanism, the engrafted cells can then exert a regenerative effect, a paracrine effect, or both[15]. In the absence of cell homing, c-kit-BMCs die by apoptosis (not shown). This peculiar aspect of cell death is termed anoikis and is triggered by the lack of cell-to-cell contact[16]. Apoptosis was restricted to the non-engrafted c-kit-BMCs which failed to express connexin 43 and N-cadherin and were unsuccessful to take residence within the myocardium. Cell death never occurred in engrafted c-kit-BMCs. At this early time point, c-kit-BMCs were frequently CD45 positive. A subset of c-kit-BMCs was CD45 negative and expressed the cardiac transcription factors GATA4 and Nkx2.5 (**Fig. 2c**). Thus, c-kit-BMCs home to the myocardium where they largely maintain the hematopoietic phenotype, although a small fraction of cells acquire rapidly the cardiomyocyte lineage.

Within 2-5 days, EGFP-positive and EGFP-negative c-kit-BMCs integrated within the host myocardium and assembled in temporary niches, which mimicked the cardiac niches[13]. Clusters of male c-kit-BMCs and male c-kit-BMCs early committed to the cardiac cell lineages were found in the myocardial interstitium. The synthesis of the gap junction channel protein connexin 43 and the calcium dependent transmembrane adhesion molecule N-cadherin was critical in the phenotypic conversion of c-kit-BMCs into cardiac progenitor cells. Connexin 43 and N-cadherin established direct communications between male c-kit-BMCs, and between male c-kit-BMCs and recipient female myocytes and fibroblasts (**Fig. 2d**), and this phenomenon was invariably

associated with the loss of bone marrow specification with lack of expression of CD45. Conversely, markers of cardiomyocytes and vascular endothelial cells (ECs) and smooth muscle cells (SMCs) were detected in some of the engrafted male c-kit-BMCs, suggesting that the myocardial microenvironment changed the fate of c-kit-BMCs. Additionally, homed cells were cycling with a 51% cumulative BrdU labeling over a period of 5 days, and a 11% expression of Ki67 at this time point. Non-engrafted male CD45-positive c-kit-BMCs died by apoptosis and were hardly detectable at 5 days after implantation. Thus, c-kit-BMCs engraft, survive and grow within the myocardium by forming junctional complexes among them and with resident myocytes and fibroblasts.

Gap junctions and destiny of BMCs

An important question concerns the role that the formation of gap junctions between c-kit-BMCs and myocytes may have in the fate of BMCs. In fact, the translocation of calcium from myocytes to c-kit-BMCs via gap junctions could have profound effects on their acquisition of the myocyte lineage, growth and differentiation. For this purpose, a functional assay was performed in which cell coupling was analyzed in vitro by two-photon microscopy after preincubation and loading of c-kit-BMCs with the red fluorescent dye DiI, which integrates stably within the cell membrane[17]. Labeled c-kit-BMCs (red) were plated with rat neonatal myocytes, which were loaded with the fluorescent dye calcein[18]. The appearance of green fluorescence in c-kit-BMCs indicated the transfer of calcein from myocytes to these cells mediated by the expression of connexin 43 and the formation of gap junctions (**Fig. 3a-c**). For real time dye transfer, cascade blue was injected either in myocytes or c-kit-BMCs and the timing of the transfer of fluorescence from one cell to the other was established (**Fig. 3d-n**). When c-kit-BMCs

were loaded with rhodamine-labeled dextran, this high molecular weight dye (M.W. 70,000) did not translocate to myocytes suggesting that the transfer of calcein occurred through gap junctions (**Fig. 3o**).

Myocardial regeneration and BMCs

Three classes of c-kit-BMCs were employed to induce myocardial regeneration: **1**. Male EGFP-positive c-kit-BMCs from mice in which EGFP was under the control of the ubiquitous beta-actin promoter; **2**. Male EGFP-negative c-kit-BMCs from mice in which EGFP was under the control of the α-myosin-heavy-chain promoter, and **3**. Male EGFP-negative c-kit-BMCs from mice in which nuclear targeted Akt had a c-myc tag and was under the control of the α-myosin-heavy-chain promoter. Therefore, all cells generated by the differentiation of the first category of c-kit-BMCs had to express EGFP while, in the second case, only the myocytes derived from the commitment of the c-kit-BMCs would acquire EGFP. And in the third instance, the c-myc tag would be equally restricted to the myocytes formed by transdifferentiation of c-kit-BMCs[11]. Male cells were delivered to female infarcted mice so that cell genotyping would also allow the distinction between endogenous resident cells and cells formed from differentiation of donor BMCs.

The engraftment into the myocardium of BMCs shortly after their delivery was followed by a significant degree of myocardial growth within the infarct that expanded progressively from 5 to 10 and 30 days after cell implantation (**Fig. 4a-c**). The band of regenerated myocardium was invariably located within the mid-portion of the infarcted ventricle and its presence had two critical positive consequences on cardiac remodeling; it markedly attenuated the inflammatory response associated with the acute-subacute

evolution of the infarct at 5-10 days and it prevented largely scar formation with infarct healing at 30 days. At the three time points, the myocytes and vascular ECs and SMCs located within the band of newly formed myocardium expressed the different transgenes in the anticipated fashion. The BMCs obtained from EGFP transgenic mice generated a myocardium in which cardiomyocytes, ECs and SMCs were mostly EGFP-positive. When EGFP or the c-myc tag was regulated by α-myosin-heavy-chain, the transgenes were detected exclusively in myocytes (**Fig. 4d-f**). The recognition of the Y-chromosome, however, allowed us to document that the vascular structures were also the result of BMC transdifferentiation (**Fig. 4g**). Because BrdU was injected daily, most of the new myocytes and coronary resistance arterioles and capillary profiles were labeled by BrdU, confirming their formation after the injection of c-kit-BMCs.

Further documentation of the bone marrow origin of the regenerated myocardium was obtained by the detection of DNA sequences of EGFP and c-myc by PCR in mice treated with BMCs isolated from animals in which EGFP was regulated by the β-actin promoter or from mice where EGFP and c-myc were placed under the control of the α-myosin heavy chain promoter. Genomic DNA was extracted from the regenerated infarcted myocardium and bands of expected molecular weight were identified and sequenced (**Fig. 4h-m**). Thus, adult c-kit-BMCs retain a high level of developmental plasticity; they acquire the cardiomyogenic and coronary vascular lineages and regenerate infarcted myocardium.

Myocytes and BMCs

In all cases, the regenerated myocardium contained new myocytes that expressed GATA4, Nkx2.5, MEF2C, α-sarcomeric actin, troponin I, α-actinin, and desmin.

Connexin 43 and N-cadherin that are the junctional proteins responsible for electrical and mechanical coupling were present at 5 days, but were more apparent at 10 and 30 days (**Fig. 4e**). The presence of EGFP, c-myc, and Y-chromosome offered the unequivocal documentation of the origin of these myocytes from the BMCs. The new myocytes were predominantly mononucleated with a small fraction of binucleated cells. The proportion of binucleated myocytes increased at one month (**Fig. 5a**) but was still significantly lower than that present in the adult myocardium; resident myocytes were ~95% binucleated and ~4% mononucleated, which is typical of the mouse heart[19]. Only one X- and one Y-chromosome were found in the new myocytes whereas the survived myocytes possessed two X-chromosomes. Additionally, EGFP-positive myocytes derived from EGFP-negative BMCs were isolated and shown to possess contractile activity (**Fig. 5b-f**). These observations documented that BMC transdifferentiation resulted in the generation of myocytes which were functionally competent and contributed to ventricular performance.

Additionally, the differentiation of BMCs into myocytes was assessed by the changes in mRNA and protein levels of EGFP and c-myc by real-time RT-PCR and Western blotting, respectively. In these cases, the analysis was performed in mice treated with BMCs isolated from animals in which EGFP and c-myc were modulated by the α-myosin heavy chain promoter. Because of this promoter, the expression of the two transgenes paralleled the expression of the contractile protein α-myosin heavy chain. The EGFP transcript was expressed at 5, 10 and 30 days after infarction, documenting that BMC-derived cardiomyocytes were present at all time-points (**Fig. 5g**). The RT-PCR products had the expected molecular weight their nucleotide sequences demonstrated the specificity of the assay (**Supplementary Fig. 5h**). Similarly, the presence of the EGFP

and c-myc proteins was detected in the infarcted-regenerated myocardium of treated animals at all time intervals (**Fig. 5i**). Thus, BMCs defeat lineage fidelity and adopt the myogenic fate in the absence of cell fusion creating a chimeric heart composed of male and female parenchymal cells.

Paracrine effects of BMCs

The possibility that c-kit-BMCs do not transdifferentiate but lead to an improvement in ventricular function after infarction by activating the growth and differentiation of resident CPCs or by inducing angiogenesis through the recruitment of circulating BMCs has repeatedly been suggested[20,21]. However, with some exceptions[5], the actual documentation of this interesting hypothesis has been elusive. Whether this paracrine effect is exerted by circulating BMCs that home to the myocardium or by BMCs directly injected within the heart, cells have to engraft and form junctional complexes with the recipient organ and its cellular compartments before any function can be promoted[14,15]. As shown here, c-kit-BMCs locally delivered to the border zone of the infarcted heart generate temporary niches and subsequently create *de novo* myocardium. Therefore, we tested whether the formation of resident female myocytes and coronary vessels within the surviving female myocardium was increased in the region bordering and remote from the infarct. Since BrdU was given to the animals throughout the experimental periods, newly formed structures generated by the stimulation of endogenous mechanisms had to be female in origin, positive for BrdU and negative for EGFP and c-myc.

The three classes of c-kit-BMCs had similar effects on the surviving myocardium of the infarcted heart. In all cases, newly formed myocytes and coronary capillaries were found in the adjacent and distant myocardium but the extent of myocyte and vessel

formation was comparable to that measured in untreated infarcted mice at 5, 10 and 30 days after coronary occlusion (**Fig. 6a**). Moreover, the degree of cell replication at sacrifice was determined in these two anatomical regions by Ki67 and MCM5 labeling. Again, comparable values were obtained in cell-treated and untreated infarcted mice (**Fig. 6b and 6c**). Thus, our observations are not consistent with a paracrine effect of BMCs on resident CPCs, myocytes or coronary vessels after infarction.

Ventricular function and BMCs

An important issue to be resolved concerned whether treatment with BMCs has beneficial effects on the anatomy and function of the infarcted ventricle. Ventricular dilation and wall thinning that typically develop with ischemic heart failure are major determinants of the increase in ventricular loading and the deterioration of cardiac performance after infarction[22,23]. In comparison with untreated mice, the three groups of mice which received c-kit-BMCs, showed a smaller increase in left ventricular diastolic chamber diameter (LVCD) and volume (LVCV), and a smaller decrease in infarct thickness, wall thickness-to-chamber radius ratio and ventricular mass-to-chamber volume ratio at 30 days (**Fig. 6d**).

Importantly, sequential echocardiographic analysis documented that myocardial regeneration restored contractile function in the infarcted portion of the wall (**Fig. 6e**). Hemodynamic measurements at sacrifice indicated that in treated infarcted mice cardiac repair was associated with an increase in developed pressure and + and – dP/dt at 30 days (**Fig. 6f**). Thus, BMC treatment restores a noticeable level of contraction in the regenerated myocardium increasing ventricular performance.

Discussion

The results of the current study indicate that a category of adult cells from the bone marrow shares the kind of developmental plasticity commonly seen in embryonic stem cells; c-kit-BMCs engraft in proximity of the damaged area of the heart and differentiate into cells of the cardiogenic lineage forming a functionally competent myocardium composed of myocytes and coronary vessels. The regenerated myocardium positively interferes with the development of the post-infarction myopathy, attenuating the dramatic changes in ventricular size and shape and the progressive deterioration in cardiac function which occur chronically after infarction[22,23]. Our data strongly suggest that adult c-kit-BMCs integrate within the host myocardium where they establish temporary niches which create the microenvironment necessary for the engrafted cells to acquire the cardiac fate and subsequently form *de novo* myocardium. These observations are particularly important because small double blind multi-center clinical trials in which mononuclear BMCs have been administered to patients with acute and chronic ischemic heart failure have recently been completed[24,25]. In spite of the positive results, the mechanism by which mononuclear BMCs improve the outcome of acute myocardial infarction and chronic ischemic cardiomyopathy in humans remains unclear. Moreover, effort is being made to initiate large trials regardless of the uncertainties about the actual effects of mononuclear BMCs on the decompensated heart. However, our results suggest that myocardial regeneration is a likely possibility.

The local injection of BMCs from transgenic mice, in which the transgene construct EGFP or c-myc was myocyte restricted, led to a time dependent increase in the

generation of myocytes and vascular structures. Thus, BMCs homed to the myocardium where they lost the hematopoietic fate and adopted the cardiac destiny forming new myocytes which participated in ventricular function. Together, the present results suggest that progenitor cells resident in the bone marrow and in the heart share a core of "stemness" genes that regulate their undifferentiated state and self-renewal properties. But each progenitor cell class expresses tissue-restricted genes that may determine the efficiency of differentiation into organ specific lineages.

The early studies on BMCs and cardiac repair[3] have been followed by numerous negative reports which have rejected the notion of stem cell plasticity and the relevance of BMCs for the management of the human disease[6-9]. The therapeutic potential of BMCs was questioned at multiple levels and the possibility of cell fusion was introduced as the actual mechanism of tissue repair[26,27]. The documentation that BMCs fuse with resident cardiomyocytes is technically demanding. This involves the identity of the fused cell, the functional competence of the progeny, the recognition of the fusion partner and the demonstration that the converted cell is a hybrid[28]. The fate of BMCs following their injection in injured organs has been characterized with the Cre-Lox genetic system. Unfortunately, the Cre-Lox model cannot exclude that metabolic cooperation occurs between the progenitor cell carrying the Cre-recombinase and the recipient cardiac cell. Because of the small molecular weight of the Cre-recombinase, this enzyme can translocate *via* gap junction channels[29] or nanotubules[30] to the resident cells mimicking cell fusion[28]. Therefore, we have excluded cell fusion by measuring the number of sex chromosomes in the preexisting and newly formed cells by the FISH assay. The new cardiomyocytes were functionally competent and were significantly smaller than the host

cells further excluding fusion events. In this regard, no viable partner cells are available for fusion in transmural myocardial infarcts. Importantly, fusion history may be concealed by the occurrence of reductive mitosis[31] in which the fused cell would expel part of its chromosomal DNA and convert a tetraploid cell into a diploid cell, masking the formation of a heterokaryon. However, there is no demonstration of this unusual cell behavior either in vitro or in vivo.

More recently, the possibility that BMC therapy of the infarcted heart exerts its beneficial effects by the activation of resident progenitor cells located in the surviving myocardium has been claimed[10]. According to this hypothesis, BMCs may contribute indirectly to cardiac regeneration by releasing a variety of peptides that exert a paracrine action on the myocardium and its resident progenitor cells. Although the current work does not support this indirect role of BMCs in cardiac repair, positive and negative results have been obtained[5,20,21,32]. The most convincing example in favor of the paracrine effect of hematopoietic cells has been found with a novel human bone marrow stem cell[5]. This unique primitive cell induces the formation of myocytes and coronary vessels within the infarcted heart and promotes a robust regenerative response in the surviving myocardium. Thus, these findings point to the notion that BMCs adopt the cardiac phenotype and potentiate the growth reserve of the adult heart. Collectively, these observations emphasize the therapeutic import of BMCs for cardiac diseases in humans.

References

1. Tosh, D., & Slack, J.M. How cells change their phenotype. *Nat Rev Mol Cell Biol.* **3**, 187-194 (2002).

2. Harris, R.G. *et al.* Lack of a fusion requirement for development of bone marrow-derived epithelia. *Science*. **305**, 90-93 (2004).

3. Orlic, D. *et al.* Bone marrow cells regenerate infarcted myocardium. *Nature.* **410**, 701-705 (2001).

4. Lanza, R., Regeneration of the infracted heart with stem cells derived by nuclear transplantation. *Circ Res.* **94**, 820-827 (2004).

5. Yoon, Y.S. *et al.* Clonally expanded novel multipotent stem cells from human bone marrow regenerate myocardium after myocardial infarction. *J Clin Invest.* **115**, 326-338 (2005).

6. Murry, C.E. *et al.* Haematopoietic stem cells do not transdifferentiate into cardiac myocytes in myocardial infarcts. *Nature.* **428**, 664-668 (2004).

7. Balsam, L.B. *et al.* Haematopoietic stem cells adopt mature haematopoietic fates in ischaemic myocardium. *Nature.* **428** , 668-673 (2004).

8. Nygren, J.M. *et al.* Bone marrow-derived hematopoietic cells generate cardiomyocytes at a low frequency through cells fusion, but not transdifferentiation. *Nat Med.* **10**, 494-501 (2004).

9. Chien, K.R. Stem cells: lost in translation. *Nature.* **428**, 607-608 (2004).

10. Chien, K.R. Lost and found: cardiac stem cells therapy revisited. *J Clin Invest.* **116**, 1838-1840 (2006).

11. Tsujita, Y. *et al.* Nuclear targeting of Akt antagonizes aspects of cardiomyocyte hypertrophy. *Proc Natl Acad Sci USA.* **103**, 11946-11951 (2006).

12. Alivisatos, A.P., Gu, W., & Larabell, C. Quantum dots as cellular probes. *Annu Rev Biomed Eng.* **7**, 55-76 (2005).

13. Urbanek, K. *et al.* Stem cells niches in the adult mouse heart. *Proc Natl Acad Sci USA.* **103**, 9226-9231 (2006).

14. Lapidot, T., Dar, A., & Kollet, O. How do stem cells find their way home? *Blood*. **106**, 1901-1910 (2005).

15. Scadden, D.T. The stem-cell niche as an entity of action. *Nature.* **441**, 1075-1079 (2006).

16. Melendez, J. *et al.* Cardiomyocyte apoptosis triggered by RAFTK/pyk2 via Src kinase is antagonized by paxillin. *J Biol Chem.* **279**, 53516-53523 (2004).

17. Czyz, J., Irmer, U., Schulz, G., Mindermann, A., & Hulser, D.F. Gap-junctional coupling measured by flow cytometry. *Exp Cell Res.* **255**, 40-46 (2000).

18, Cancelas, J.A., *et al.* Connexin-43 gap junctions are involved in multiconnexin-expressing stromal support of hemopoietic progenitors and stem cells. *Blood.* **96**, 498-505 (2000).

19. Limana, F. *et al.* bcl-2 overexpression promotes myocyte proliferation. *Proc Natl Acad Sci USA.* **99**, 6257-6262 (2002).

20. Mangi, A.A. *et al.* Mesenchymal stem cells modified with Akt prevent remodeling and restore performance of infarcted hearts. *Nat Med.* **9**, 1195-1201 (2003).

21. Amado, L.C. *et al.* Cardiac repair with intramyocardial injection of allogeneic mesenchymal stem cells after myocardial infarction. *Proc Natl Acad Sci USA.* 102, 11474-11479 (2005).

22. Pfeffer, M. A., & Braunwald, E. Ventricular remodeling after myocardial infarction. Experimental observations and clinical implications. *Circulation.* **81**, 1161-1172 (1990).

23. Opie, L.H., Commerford, P.J., Gersh, B.J., & Pfeffer, M.A. Controversies in ventricular remodeling. *Lancet.* **367**, 356-67 (2006).

24. Schachinger V. *et al.* Intracoronary bone-marrow derived progenitor cells in acute myocardial infarction. *N Engl J Med.* **355**, 1210-1221.

25. Assmus, B. *et al.* Transcoronary transplantation of progenitor cells after myocardial infarction. *N Engl J Med.* **355**, 1222-1232.

26. Wagers, A.J., Sherwood, R.I., Christensen, J.L., & Weissman, I.L. Little evidence for developmental plasticity of adult hematopoietic stem cells. *Science.* **297**, 2256-2259 (2002).

27. Wagers, A.J., & Weissman, I.L. Plasticity of adult stem cells. *Cell.* **116**, 639-648 (2004).

28. Leri, A., Kajstura, J. & Anversa, P. Cardiac stem cells and mechanisms of myocardial regeneration. *Physiol Rev.* **85**, 1373-1416 (2005).

29. Subak-Sharpe, H., Burk, R.R., & Pitts, J.D. Metabolic cooperation between biochemically marked mammalian cells in tissue culture. *Rev Med Virol.* **12**, 69-78 (1969).

30. Koyanagi, M., Brandes, R.P., Haendeler, J., Zeiher, A.M., & Dimmeler, S. Cell-to-cell connection of endothelial progenitor cells with cardiac myocytes by nanotubes: a novel mechanism for cell fate changes? *Circ Res.* **96**, 1039-1041 (2005).

31. Wang, X. *et al.* Cell fusion is the principal source of bone-marrow-derived hepatocytes. *Nature.* **422**, 897-901 (2003).

32. Kajstura, J. *et al.* Bone marrow cells differentiate in cardiac cell lineages after infarction independently of cell fusion. *Circ Res*. **96**, 127-137 (2005).

Legends to Figures

Figure 1. Autofluorescence and quantum dots. a, The excitation and emission wavelengths of the semiconductor particles Qdot 655 are distinct from the autofluorescence wavelength of tissue sections. The dotted line indicates the excitation wavelength for blue diode laser and Qdots, 405 nm, and the red line shows the emission wavelength of Qdot 655. The black line illustrates the spectrum of autofluorescence for formalin-fixed tissue sections. **b-d,** The confocal image illustrated in panels **b** was acquired with an emission wavelength of 525 nm while those shown in panels **c** and **d** were obtained with an emission wavelength of 655 nm. Nuclei in panel **b-d** are stained by DAPI which binds directly to DNA and does not require antibody labeling. Autofluorescence is detected only at 525 nm (**b**, green) while it is not present at 655 nm (**c**). The same field is shown in panel **d** after immunolabeling with α-sarcomeric actin (red) antibody conjugated with Qdot 655. **e-h,** TRITC fluorescence undergoes rapidly photobleaching as documented by the decay in the intensity of the signal after 10 minutes of exposure to the laser light of the confocal microscope (**e**, **f**). Quantum dots are resistant to photobleaching; intensity of labeling and structural detail is preserved after 10 minutes (**g**, **h**).

Figure 2. BMCs from EGFP transgenic mice form niches in the infarcted myocardium. a, **b**, One day after infarction and injection of c-kit-positive-BMCs, the implanted cells engraft within the myocardium and are connected to myocytes (red, α-sarcomeric actin) and fibroblasts (magenta, procollagen) by connexin 43 (**a**, yellow, arrowheads) and N-cadherin (**b**, yellow, arrowheads). BMCs express EGFP (green). **c**, BMCs that undergo myocyte differentiation lose the pan-leukocyte marker CD45 (white,

arrows) and express Nkx2.5 (magenta dots, arrowheads). **d**, Five days after myocardial infarction, the engrafted BMCs express c-kit (green) and form temporary niches; gap junctions (connexin 43, yellow, arrowheads) are apparent between myocytes (red, α-sarcomeric actin) and fibroblasts (magenta, procollagen) and the c-kit-positive-BMCs. c-kit-BMCs have a male genotype (Y-chromosome, white dots, arrows).

Figure 3. c-kit-BMCs are functionally connected with cardiomyocytes. a-c, These images were obtained by two-photon microscopy. Sorted c-kit-positive BMCs were loaded with DiI (**a**, red fluorescence) and cocultured with neonatal myocytes labeled with calcein (**b**, green fluorescence). The appearance of green-fluorescence in c-kit-BMCs (**c**, yellow-green fluorescence, arrowheads) demonstrates the translocation of calcein from myocytes to c-kit-BMCs. **d-o**, These images were obtained by epifluorescence (**d, f-j, l-o**) and phase-contrast microscopy (**e, k**). EGFP-positive c-kit-BMCs (**d**, **j**, green) were co-cultured with neonatal rat myocytes (**e**, **k**, dotted lines) and impaled with a micropipette filled with cascade blue (**f**, **l**, arrows). Images represent the real-time transfer of cascade blue from c-kit-BMCs to myocytes. Note the appearance of the fluorescent dye in the myocytes adjacent to the c-kit-BMCs (**h**, **i**, **n**, dotted lines). Red fluorescence in **o** depicts the lack of translocation of rhodamine-labeled dextran from the c-kit-BMC to the adjacent myocyte.

Figure 4. Myocardial regeneration after infarction is mediated by the injection of c-kit-BMCs. a-c, Areas of regenerated myocardium within the infarcted left ventricular wall, included between the epimyocardium (EP) and the endomyocardium (EN) at 5 (**a**), 10 (**b**) and 30 (**c**) days after coronary occlusion. The presence of c-myc (green) in the newly formed myocytes (red, α-sarcomeric actin) documents their bone marrow origin.

Arrowheads delimit the areas of regenerated myocardium. **d**, Myocardium of α-MHC-nuc-Akt mouse was employed as positive control for c-myc staining (green); only myocyte nuclei express the c-myc tag (arrowheads). **e-g**, These higher magnifications illustrate newly formed myocytes carrying the c-myc tag (**e**, **f**, green) or the Y-chromosome (**g**, white dots in nuclei). New myocytes are connected by gap junctions (**e**, connexin 43, yellow dots; arrowheads). Two newly formed arterioles are also evident in the regenerated myocardium (**f**, **g**). Smooth muscle cells express α-smooth muscle actin (**f**, **g**, yellow) and Y-chromosome (**g**, white dots). Newly formed myocytes and smooth muscle cells (**g**) contain at most one X- (green) and one Y-chromosome (white). The periphery of the cells is defined by laminin (**d-f**, white).

h-j, Detection of mouse DNA for EGFP and c-myc in the regenerated infarcted myocardium (MI) and surviving myocardium (SM) of hearts injected with c-kit-BMCs obtained from β-actin-EGFP (**h**), αMHC-EGFP (**i**) and αMHC-nuc-Akt (**j**) transgenic mice. DNA extracted from the tails of the three transgenic animals was employed as positive control (+). WT, wild type mouse. LB, lysis buffer incubated with primers in the absence of DNA template. **k-m**, The nucleotide sequences of the PCR products was established in the sense and antisense direction to confirm the specificity of the amplified bands. NLS, nuclear localization signal.

Figure 5. The regenerated myocytes are functionally competent. a, Only small fractions of regenerated myocytes were binucleated. Results are mean±SD. *Indicates a difference vs 5 and 10 days. **b-f**, Myocytes were isolated from the infarcted-regenerated myocardium 15 days after the injection of c-kit-BMCs from αMHC-EGFP transgenic mice. Newly formed myocytes are EGFP-positive while surviving myocytes are EGFP-

negative (**b**, **c**). **d**, Phase contrast image of a contracting myocyte. Cell shortening is shown in panel **e** by EGFP fluorescence and in panel **f** by changes in myocyte length.

Figure 6. Myocardial regeneration, cardiac anatomy and function. a-c, Myocyte and endothelial cell (EC) proliferation in the surviving myocardium of untreated (UN) and treated (TR) mice. The values in the three groups of treated mice were similar and were combined. Results are mean±SD. **d**, Effects of myocardial regeneration on the anatomy of the infarcted heart. Results are mean±SD. *Indicates a difference vs sham-operated mice (SO) and **indicates a difference vs untreated mice (UN). TR, treated mice. **e**, The echocardiogram shows the lack of contraction in the infarcted region of the wall of an untreated heart (arrows) and the reappearance of contraction (arrowheads) in the infarcted wall of a heart treated with c-kit-BMCs obtained from αMHC-nuc-Akt transgenic mice. The mid panel and lower panel correspond to the same heart analyzed at 16 and 30 days after cell injection, respectively. **f**, Effects of myocardial regeneration on the function of the infarcted heart. Results are mean±SD. *Indicates a difference vs sham-operated mice (SO) and **indicates a difference vs untreated mice (UN). TR, treated mice. **g**, Expression of EGFP mRNA in the infarcted-regenerated myocardium of treated mice by quantitative RT-PCR. **h**, Nucleotide sequences in sense and antisense directions of the RT-PCR products. **i**, Expression of EGFP and c-myc proteins in the infarcted-regenerated myocardium of treated mice by Western blotting. The hearts of wild type and transgenic mice were used as negative and positive controls, respectively.

Methods

In vivo studies

Isolation of bone marrow cells (BMCs). Three transgenic mouse models were employed as donors of c-kit-positive BMCs (c-kit-BMCs): male mice expressing EGFP under the control of the ubiquitous β-actin promoter (β-actin-EGFP); male mice expressing EGFP under the control of the α-myosin heavy chain promoter (αMHC-EGFP); and male mice in which nuclear targeted Akt fused with a c-myc tag was placed under the control of the α-myosin heavy chain promoter (αMHC-nuc-Akt). Bone marrow was harvested from the femurs and tibias and cells were suspended in PBS containing 5% fetal calf serum. BMCs were then incubated with a CD117 microbeads and enriched for c-kit[1] by immunomagnetic cell sorting (Miltenyi Biotec). For intramyocardial injection, freshly isolated c-kit-BMCs were suspended at a concentration of 6 x 10^4 cells in 6 μl PBS containing polystyrene microspheres conjugated with rhodamine (Molecular Probes) for the recognition of the site of injection[1,2].

Myocardial infarction

Myocardial infarction was induced in anesthetized (ketamine 150 mg/kg body weight, acepromazine 0.85 mg/kg body weight) female wild type mice at ~3 months of age as previously described[1-4]. Because of differences in the genetic background of the donors, c-kit-BMCs from β-actin-EGFP mice were injected in C57BL/6 mice while c-kit-BMCs from αMHC-EGFP and αMHC-nuc-Akt were injected in FVB/N mice. Shortly after coronary occlusion, two injections each of 3.0 μl of PBS containing 30,000 c-kit-BMCs were performed in the anterior and posterior aspects of the viable myocardium bordering the infarct. After the collection of hemodynamic data, mice were sacrificed at 12-36

hours, and at 2, 5, 10 and 30 days after surgery. Sham-operated and infarcted mice injected with PBS or glutaraldehyde-fixed c-kit-BMCs and rhodamine particles were used as controls. Additionally, all animals were injected twice a day with BrdU, 50 mg/kg body weight intraperitoneally. Animal protocols were approved by the Institutional Review Board.

Echocardiography and ventricular function. Echocardiographic parameters were collected in conscious mice at 10 and 30 days after infarction by using a Sequoia 256c (Acuson) equipped with a 13-MHz linear transducer (15L8). The anterior chest area was shaved and two- dimensional (2D) images and M-mode tracings were recorded from the parasternal short axis view at the level of papillary muscles. From M-mode tracings, anatomical parameters in diastole and systole were obtained[1,2,4,5]. Before sacrifice, mice were anesthetized with chloral hydrate (400 mg/kg body weight, i.p.), and a microtip pressure transducer (SPR-671; Millar Instruments) connected to a recorder (iWorx214) was advanced into the LV for the evaluation of LV pressures and LV + and − dP/dt in the closed-chest preparation[1-5].

Cardiac anatomy and infarct size. After hemodynamic measurements, the abdominal aorta was cannulated with a polyethylene catheter filled with phosphate buffer, 0.2 M, pH 7.4, and heparin, 100 units/ml. In rapid succession, the heart was arrested in diastole by the injection of $CdCl_2$, 100 mM, through the aortic catheter, the thorax opened, perfusion with phosphate buffer started and the vena cava cut to allow drainage of blood and perfusate[1-5]. The aortic catheter was connected to a pressure reservoir to adjust perfusion pressure to mean arterial blood pressure measured *in vivo*. Simultaneously, the LV chamber was filled with fixative, 10% formalin in phosphate buffer, from a pressure

reservoir set at a height equivalent to end-diastolic pressure determined in vivo. This was accomplished by inserting a 25G3/4 needle connected to the pressure reservoir into the LV through the apex. After perfusion with buffer for 2 min, the coronary vasculature was perfused for 15 min with fixative. Subsequently, the heart was excised and weights recorded. The volume of the myocardium was determined[6] by dividing the weight by the specific gravity of muscle tissue, 1.06 g/ml. After paraffin embedding, three tissue sections, from the base to the apex of the left ventricle, were stained with hematoxylin and eosin. The mid-section was used to measure LV thickness, chamber diameter, and volume[1-6]. Infarct size was assessed by the fraction of myocytes lost from the LV[1-6].

Regenerated myocardium. The newly formed myocardium within the infarcted heart was identified by the detection of EGFP in animals injected with c-kit-BMCs from β-actin-EGFP mice. However, in animals treated with c-kit-BMCs from αMHC-EGFP and αMHC-nuc-Akt mice, both EGFP and c-myc were restricted to myocytes. Therefore, the detection of the Y-chromosome was employed to recognize not only myocytes but also vascular endothelial cells (ECs) and smooth muscle cells (SMCs).

Cell differentiation, proliferation and death. For the recognition of cell differentiation, the expression of membrane, cytoplasmic and nuclear proteins specific of myocytes, ECs and SMCs were evaluated. Labeling by BrdU, Ki67 and MCM5 was employed to evaluate cycling cells while apoptosis was determined by the TdT assay[7-9]. These measurements were obtained by confocal microscopy and the antibodies employed and the modalities of labeling are listed in **Table 1**.

X and Y chromosomes. For the FISH assay[1,8,9], sections were exposed to a denaturating solution containing 70% formamide. After dehydration with ethanol, sections were

hybridized with the mouse Whole Chromosome-Specific Probes for Y and X-chromosomes (Cambio). Nuclei were stained with propidium iodide.

PCR for detection of EGFP and c-myc DNA. This DNA analysis was performed in the three groups of infarcted mice treated with c-kit-BMCs obtained from β-actin-EGFP, αMHC-EGFP and αMHC-nuc-Akt mice. Tissue sections, in which myocardial regeneration was detected by immunohistochemistry, were subjected to deparaffinization for 30 min at 70°C and subsequently were immersed in xylene and ethanol at decreasing concentration. Slides were then washed in distilled water. The regenerated infarcted myocardium and the surviving myocardium were removed from the slides and genomic DNA was extracted with the QIAamp DNA micro kit (Qiagen). DNA, 100 ng, was mixed with primers for EGFP or c-myc. For EGFP, eGFP-F: 5'-ATGGTGAGCAAGGGCGAG-GAGCTG-3' and eGFP-R:5'-GCCGTCGTCCTTGAAGAAGATGGTG-3' were used. Cycling conditions were as follows: 94°C for 30 sec, followed by 30 cycles of amplification (94°C for 30 sec, 62°C for 30 sec, 72°C for 30 sec), with a final incubation at 72°C for 3 min. For c-myc, we employed a reverse primer complementary to the c-myc sequence and a forward primer complementary to the adjacent Akt sequence: c-myc-R: 5'-CAGATCCTCTTCTGAGATGAGT-3' and Akt-F: 5'-GATGAGGAGTTCACAGCT-CAGATG-3'. Cycling conditions were: 94°C for 30 sec, followed by 35 cycles of amplification (94°C for 30 sec, 62°C for 30 sec, 72°C for 30 sec), with a final incubation at 72°C for 3 min. The final PCR products were run onto agarose gel for the detection of the EGFP and c-myc bands. For EGFP, the amplicon size was 315 bp and for c-myc, the amplicon size was 258 bp. Tails obtained from β-actin-EGFP mice and αMHC-nuc-Akt

mice were used as positive controls while tissue sections from animals injected with PBS were used as negative controls.

Real-time RT-PCR for EGFP mRNA. This analysis was performed in infarcted mice treated with c-kit-BMCs obtained from αMHC-EGFP mice sacrificed at 5, 10 and 30 days after surgery. Hearts were excised and the infarcted-regenerated area was separated from the spared myocardium and employed for RNA extraction. Total RNA was purified using RNeasy Mini kit and RNase-Free DNase Set (Qiagen) and in each sample, ~50-100 μg of RNA were collected. RNA was eluted in 100 μl of RNase-free water, and 50 μg of total RNA were employed for poly(A)RNA selection using MicroPoly(A)Purist (Ambion). Nearly 1.5-2 μg of poly(A)RNA were recovered from each sample and treated with DNase I. After heat inactivation of DNase I, 500 ng of poly(A)RNA were employed for reverse transcription (RT) into cDNA using SuperScript III cDNA synthesis kit (Invitrogen); RNA was incubated with 5'-phosphorylated oligo$(dT)_{20}$ primer for 3.5 hours at 50°C. Synthesized cDNA was treated with 2 U of RNase H (Ambion) at 37°C for 20 minutes. Real-time RT-PCR analysis was performed on 7300 Real Time PCR System (Applied Biosystems) and run in duplicate using 1/20th of the cDNA per reaction. Approximately 25 ng of poly(A)RNA were used for non-RT control reaction. Primers and probes for EGFP transgene and the housekeeping gene GAPDH were designed from available mouse sequences using the primer analysis software Primer Express v2.0 (Applied Biosystems).

The PCR-reaction included 1 μl template cDNA, 500 nM forward and reverse-primers, and 100 nM probe conjugated with the fluorescent dye FAM in a total volume of 25 μl. Cycling conditions were as follows: 95°C for 10 minutes followed by 50 cycles of

amplification (**95°C denaturation for 15 sec, and 60°C combined annealing/extension for 1 min**). FAM signal was detected at the end of each cycle. Data were analyzed using the Automatic Baseline of the Sequence Detection software (v. 1.2.2; Applied Biosystems), and the threshold was fixed at 0.05 manually for cycle threshold (Ct) determination. Quantified values were normalized against the input determined by the housekeeping mouse gene GAPDH.

Real-time RT-PCR products were run on 2% agarose/1x TBE gel. Amplified fragments were cut out and DNA was extracted using QIAquick Gel Extraction kit (Qiagen). DNA was eluted in 30 μl of 10 mM Tris buffer (pH 8.5), and amplified by Platinum Blue PCR Supermix (Invitrogen) in the presence of 260 nM of the forward and reverse primers utilized for real-time PCR. PCR reaction was carried out in Eppendorf Mastercycler. **Cycling conditions were as follows: 94°C for 2 min followed by 35 cycles of amplification (94°C denaturation for 20 sec, 60°C annealing for 30 sec, 72°C elongation for 20 sec) with a final incubation at 72°C for 3 min.** After purification using QIAquick PCR Purification kit (Qiagen), samples were submitted to the DNA Sequencing Facility at Cornell University (New York) to obtain the DNA sequence.

Western blotting for EGFP and c-myc. This analysis was performed in infarcted mice treated with c-kit-BMCs obtained from αMHC-EGFP mice and from α-MHC-nuc-Akt sacrificed at 30 days after surgery. Hearts were excised and the infarcted-regenerated area was separated from the spared myocardium and employed for protein extraction. In each sample, ~10 g of proteins were collected. Equivalents of 50 μg of proteins were loaded for each sample. Samples were runt onto 8% polyacrylamide gels. Polyclonal rabbit anti-

EGFP and polyclonal rabbit anti-c-myc were employed as primary antibodies at a concentration of 1:1,000. Anti-rabbit IgG were employed as secondary antibodies at a concentration of 1:3,000. EGFP was detected as a band of ~30 kDa and c-myc tag as a band of ~ 60 kDa.

Myocyte contractility and calcium transients. Newly formed myocytes were isolated from the infarcted region of mice treated with BMCs obtained from αMHC-EGFP mice at 15 days. Regenerated and old myocytes were discriminated by the presence and absence of EGFP, respectively. Isolated myocytes obtained from the infarcted region of treated hearts were placed in a bath on the stage of an inverted microscope. Experiments were conducted at room temperature. Cells were bathed continuously with a Tyrode solution containing (mM): NaCl 140, KCl 5.4, $MgCl_2$ 1, HEPES 5, Glucose 5.5 and $CaCl_2$ 1.0 (pH 7.4, adjusted with NaOH). Measurements were performed using IonOptix contractility systems.

In vitro studies

Isolation of BMCs and neonatal myocytes. c-kit-BMCs were isolated from wild type and β-actin-EGFP transgenic mice with the protocol described above. Myocytes were enzymatically dissociated from the heart of Sprague Dowley rats at 1 day after birth. Rats were decapitated and hearts were quickly removed and placed in Ca/Mg-free Hanks' balanced salt solution (HBSS). The tissue was cut in small pieces, which were transferred into 10 ml of dissociation medium (0.1% trypsin, 1:250, and 0.01% DNase I in HBSS) and stirred at 37°C. The material dissociated from the tissue during the first 15 minutes of trypsinization was discarded. An aliquot of dissociation medium (10 ml) was added to the remaining fragments of myocardium, and after 10 minutes of gentle stirring at 37°C the supernatant was collected. The cells contained in this fraction were centrifuged at 300 g for 4 min, resuspended in Eagle's MEM supplemented with 10% FBS and stored on ice. The procedure was repeated 4 to 6 times. Isolated cells were pre-plated in a 150-mm Petri dish for 1 hour at 37°C, and myocytes which did not attach to the dish during this time were collected[10,11].

Cell culture. C-kit-BMCs were cultured with neonatal rat myocytes in Dulbecco's MEM with 10% FBS. For dye transfer studies, living cell co-cultures were analyzed by two-photon and inverted microscopy. C-kit-BMCs were labeled with 1-2 μM of the red fluorescent dye DiI (Molecular Probes) for 5 min at 37°C and for 15 min at room temperature in Hank's solution[8]. Neonatal rat myocytes were loaded with 5 μM calcein (Molecular Probes) for 30 min at 37°C. Cells were then washed in Ca^{2+}/Mg^{2+} containing HBSS. Labeled c-kit-BMCs were cultured overnight in the presence of labeled neonatal rat cardiomyocytes. This approach was followed for the detection of functional gap

junctions between c-kit-BMCs and myocytes and dye transfer. The presence of green fluorescence in DiI-labeled cells was considered indicative of the transfer of calcein through gap junctions from myocytes to c-kit-BMCs. This analysis was performed by two-photon microscopy.

For real time dye transfer in co-cultured cells, c-kit-BMCs cells were loaded with cascade blue (1 mg/ml; Molecular Probes) by microinjection (FemtoJet, Eppendorf AG) of a medium containing (mM): K_2HPO_4, 27, $NaHPO_4$, 8, KH_2PO_4, 26 (pH 7.3). Transfer of the fluorescent dye to neighboring cells was followed by acquisition of serial images. This analysis was performed using an inverted microscope. In additional experiments, c-kit-BMCs were loaded with rhodamine-labeled dextran (10 μg/ml).

Statistical analysis. Results are presented as means ± SD. Differences were determined by the two-tailed unpaired Student's *t*-test, analysis of variance and Bonferroni method[6].

References

1. Kajstura, J. *et al.* Bone marrow cells differentiate in cardiac cell lineages after infarction independently of cell fusion. *Circ Res*. **96**, 127-137 (2005).

2. Lanza, R., Regeneration of the infracted heart with stem cells derived by nuclear transplantation. *Circ Res.* **94**, 820-827 (2004).

3. Orlic, D. *et al.* Bone marrow cells regenerate infarcted myocardium. *Nature.* **410**, 701-705 (2001).

4. Urbanek, K. *et al.* Cardiac stem cells possess growth factor-receptor systems that after activation regenerate the infarcted myocardium, improving ventricular function and long-term survival. *Circ Res.* **97**, 663-673 (2005).

5. 5. Orlic, D. *et al.* Mobilized bone marrow cells repair in infracted heart, improving function and survival. *Proc Natl Acad Sci USA.* **98**, 10344-10349 (2001).

6. Anversa, P., & Olivetti, G. Cellular basis of physiological and pathological myocardial growth. In *Handbook of Physiology Section 2: The Cardiovascular System: The Heart*, Volume 1 (eds Page, E., Fozzard, H. A., Solaro, R. J.) 75-144 (Oxford University Press, 2002).

7. Melendez, J. *et al.* Cardiomyocyte apoptosis triggered by RAFTK/pyk2 via Src kinase is antagonized by paxillin. *J Biol Chem.* **279**, 53516-53523 (2004).

8. Urbanek, K. *et al.* Stem cells niches in the adult mouse heart. *Proc Natl Acad Sci USA.* **103**, 9226-9231 (2006).

9. Urbanek, K., *et al.* Myocardial regeneration by activation of multipotent cardiac stem cells in ischemic heart failure. *Proc Natl Acad Sci USA.* **102**, 8692-8697 (2005).

10. Kajstura, J., Cheng, W., Reiss, K., & Anversa, P. The IGF-1-IGF-1 receptor system modulates myocyte proliferation but not myocyte cellular hypertrophy in vitro. *Exp Cell Res.* **215**, 273-283 (1994).

11. Cheng, W., *et al.* Downregulation of the IGF-1 system parallels the attenuation in the proliferative capacity of rat ventricular myocytes during postnatal development. *Lab Invest.* **72**, 646-655 (1995).

Table 1. Cell Markers, Function and Antibody Labeling

Cell Markers	Function	Antibody Labeling
1. BMC Epitopes and Donor Markers		
c-kit	Stem Cell Factor receptor	conjugated primary Ab
CD45	Surface Glycoprotein	primary/secondary Ab
CD34	HSC/EC antigen	conjugated primary Ab
CD45	Pan-myeloid marker	conjugated primary Ab
CD45RO	T-lymphocyte subset marker	conjugated primary Ab
CD8	T-lymphocyte subset marker	conjugated primary Ab
CD20	B-lymphocyte marker	conjugated primary Ab
TER-119	Erythroid marker	conjugated primary Ab
2. Donor BMC Markers		
EGFP	Fluorescent protein	conjugated primary Ab
c-myc	Tag sequence of Akt transgene	conjugated primary Ab
3. Junctional Proteins		
Connexin 45	Engraftment of BMCs	conjugated primary Ab
N-cadherin	Engraftment of BMCs	conjugated primary Ab

4. Transcription Factors of Cardiac Cell Lineages

GATA-4	Differentiation of cardiac cells	conjugated primary Ab
Nkx2.5	Differentiation of cardiomyocytes	conjugated primary Ab
MEF2C	Differentiation of cardiomyocytes	conjugated primary Ab
GATA-6	Differentiation of VSMCs	conjugated primary Ab
Ets1	Differentiation of ECs	conjugated primary Ab

5. Structural Proteins of Cardiac Cell Lineages

α-sarcomeric actin	Contractile protein of cardiomyocytes	conjugated primary Ab
α-actinin	Contractile protein of cardiomyocytes	conjugated primary Ab
Cardiac myosin	Contractile protein of cardiomyocytes	conjugated primary Ab
α-SM actin	Contractile protein of VSMCs	conjugated primary Ab
Von Willebrand Factor	Factor VIII receptor in ECs	conjugated primary Ab
Vimentin	Intermediate filament in ECs and Fs	primary/secondary Ab

6. Cell Proliferation

BrdU	S-phase marker	primary/secondary Ab
MCM5	cell cycle protein	primary/secondary Ab
Ki67	cell cycle marker	primary/secondary Ab

BMCs: Bone Marrow Cells; VSMCs: Vascular Smooth Muscle Cells; ECs: Endothelial Cells; Fs: Fibroblasts; Ab: Antibody.

Sources of Antibodies: **Dako**: c-kit, CD45, CD45RO, CD8; **Molecular Probes**: EGFP; **Pharmingen**: TER-119; **Roche**: BrdU; **Santa Cruz**: GATA-4, MEF2C, GATA-6, Ets1, N-cadherin, MCM5, CD34, CD20; **Sigma**: α-sarcomeric actin, connexin 43, α-smooth muscle actin, von Willebrand factor, vimentin; **Upstate Biotechnolegy**: c-myc tag; **Vector Laboratories**: Ki67;

Vorrei ringraziare in queste poche righe le persone che mi sono state accanto pur non essendolo veramente.In primis mia madre,sempre presente nella mia vita quaggiù e con lei ,la mia famiglia. Non poco sostegno dalle mie amiche di sempre Stefy e Marghe che mi hanno fatto partecipe della loro vita nonostante la mia perenne assenza.Un immenso grazie a Franca e,Tilly preziose punto di riferimento e di amicizia sincera.

Un incredibile grazie alla mia Prof. Unica nell'incoraggiarmi e sempre pronta ad ascoltarmi e farmi sentire parte del suo laboratorio anche da lontano…..

Non posso però dimenticarmi di chi mi ha sostenuto,qua.. dall'altra parte dell'oceano. Un enorme grazie a Grazia e Claudia. Compagne di avventure. Un THANK YOU per Nicole e Bobby che mi hanno sempre trattato come una sorella e sono fiera di essere tale.

Un riconoscimento senza parole per Annorosa Leri che mi ha guidato in questi mesi,sono fiera di essere qui e lavorare con lei.

Infine ringrazio di cuore il Prof Piero Anversa ,uomo geniale con un cuore di padre.

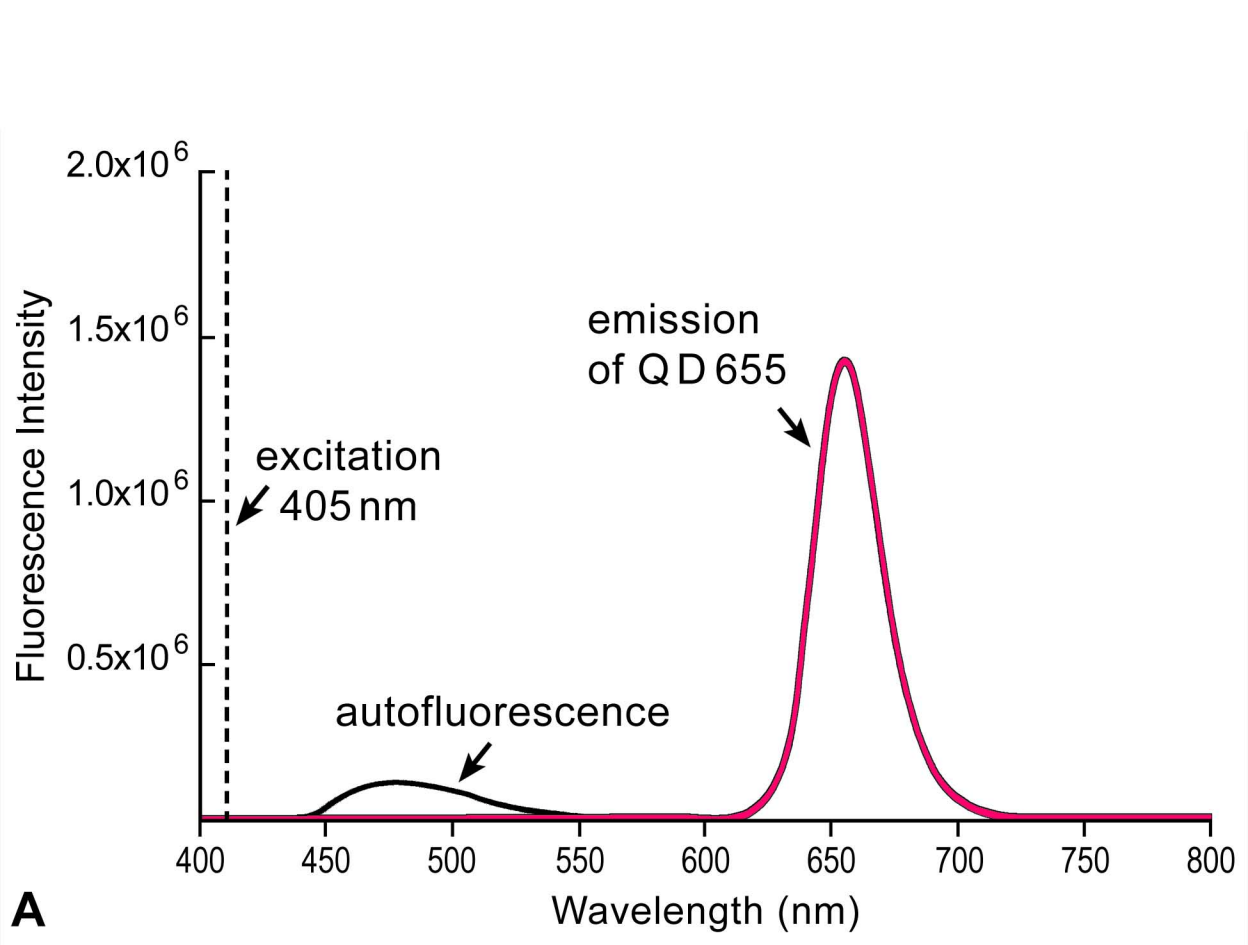
2.0x10^6
1.5x10^6
1.0x10^6
0.5x10^6
Fluorescence Intensity
emission
of Q D 655
excitation
405 nm
autofluorescence
400
450
500
550
600
650
700
750
800
Wavelength (nm)
A

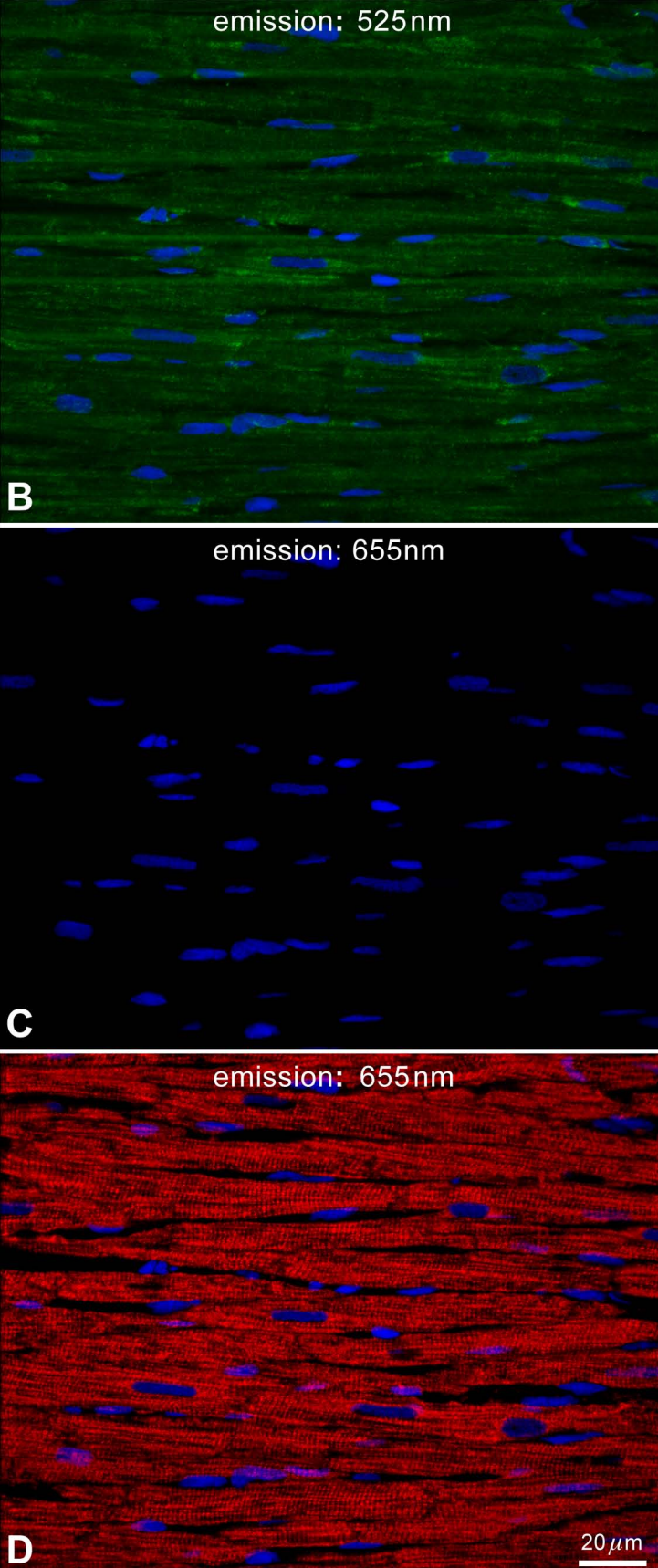
emission: 525nm
B
emission: 655nm
C
emission: 655nm
D
20 μm

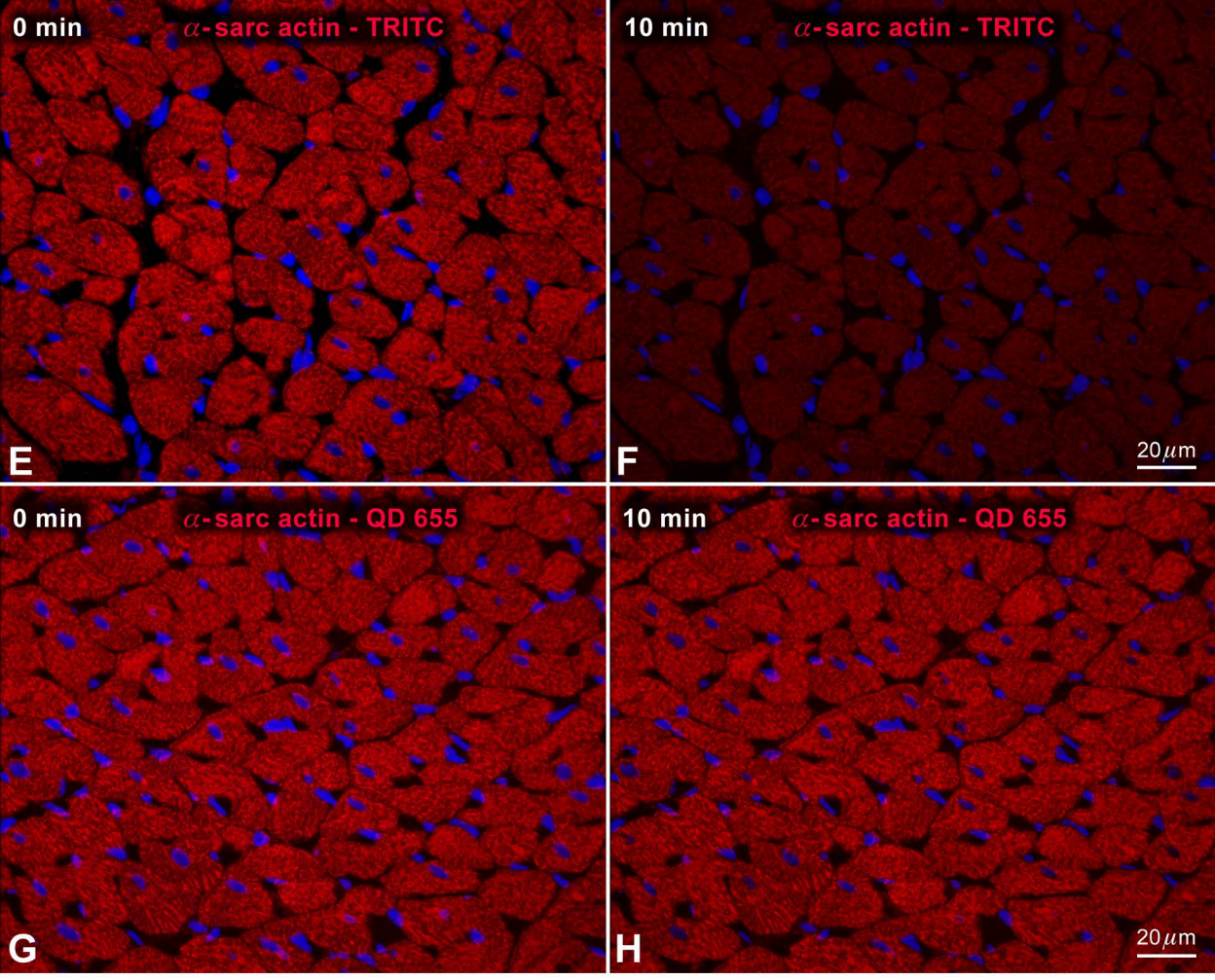
0 min
α-sarc actin - TRITC
E
10 min
α-sarc actin - TRITC
F
20μm
0 min
α-sarc actin - QD 655
G
10 min
α-sarc actin - QD 655
H
20μm

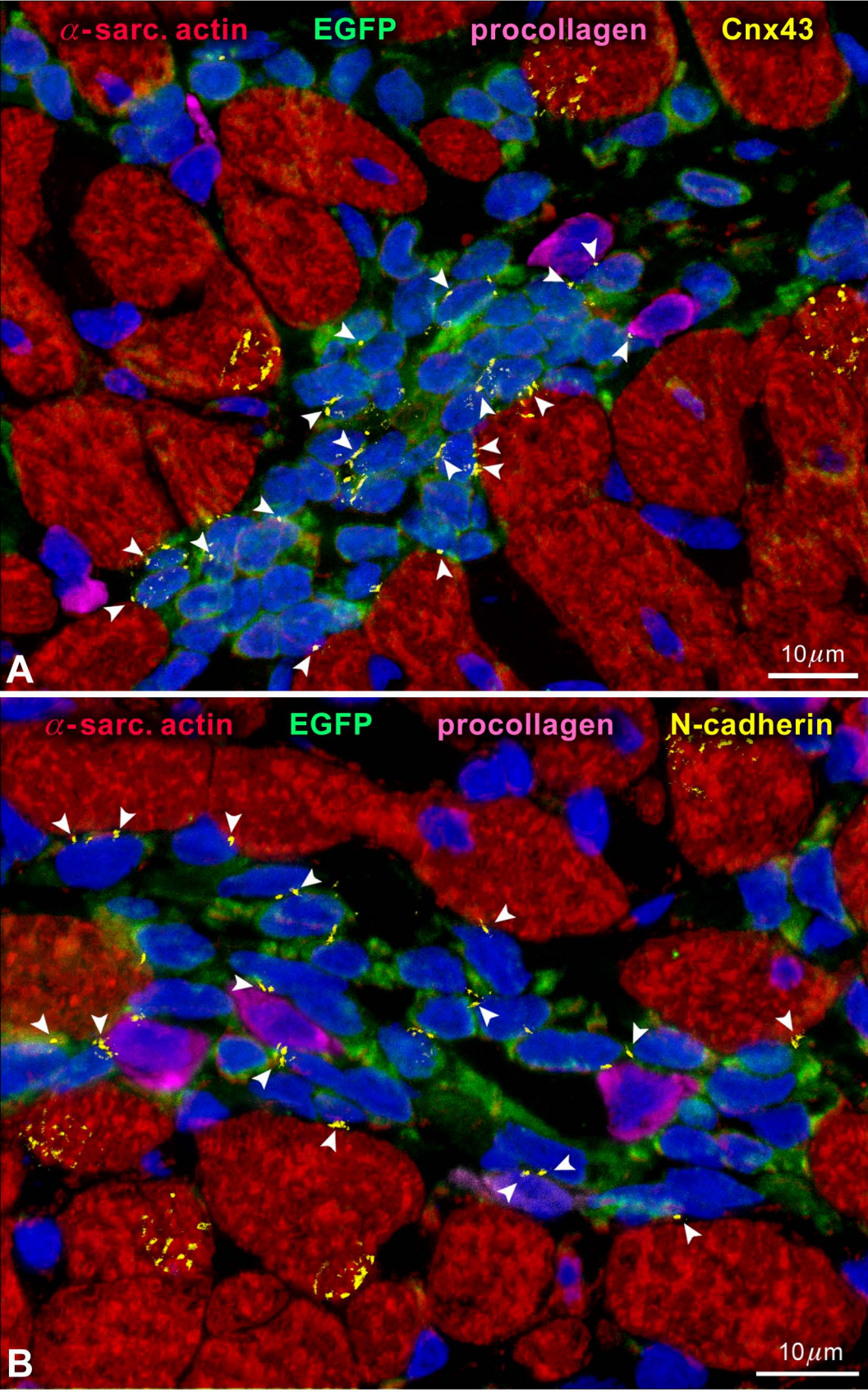
α-sarc. actin
EGFP
procollagen
Cnx43
A
10μm
α-sarc. actin
EGFP
procollagen
N-cadherin
B
10μm

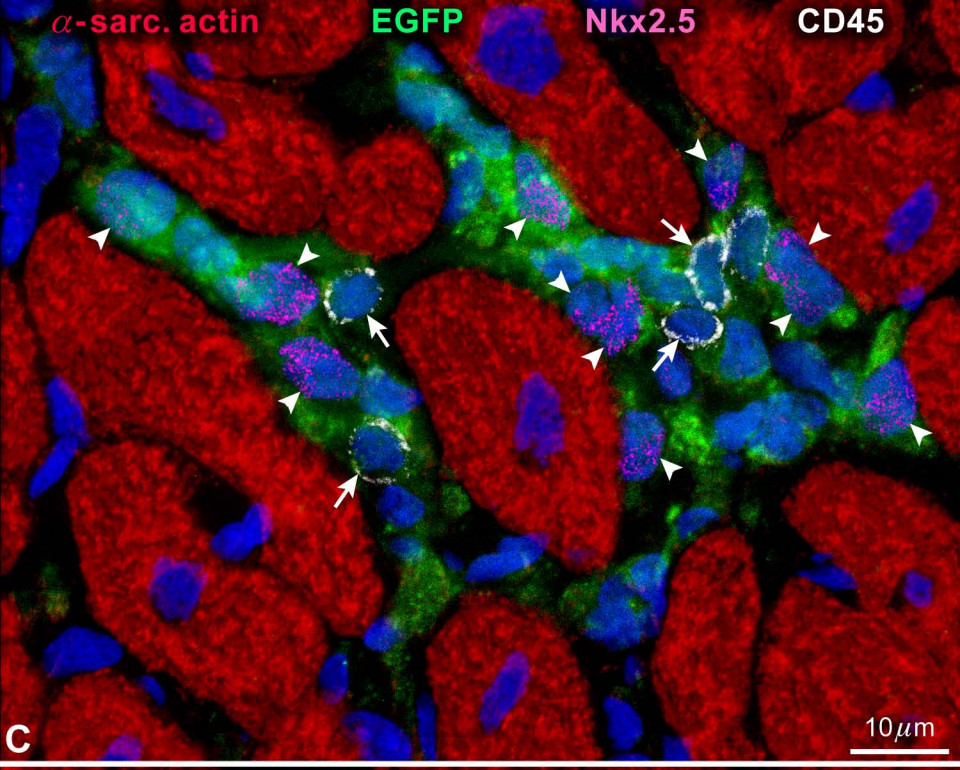
α-sarc. actin
EGFP
Nkx2.5
CD45
C
10μm

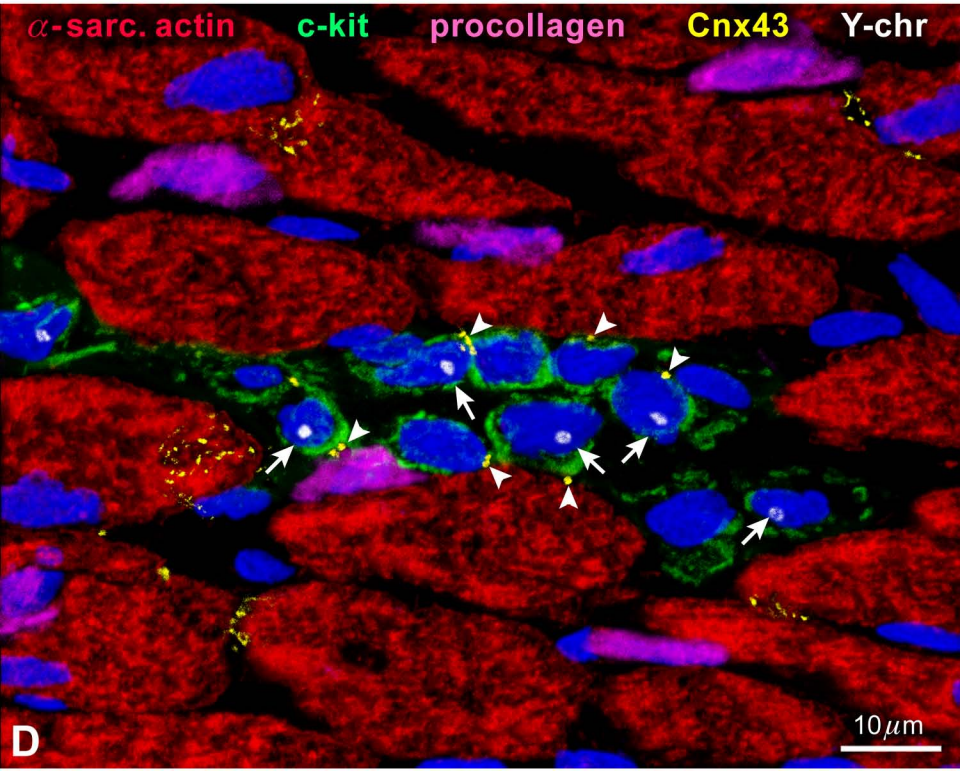
α-sarc. actin
c-kit
procollagen
Cnx43
Y-chr
D
10μm

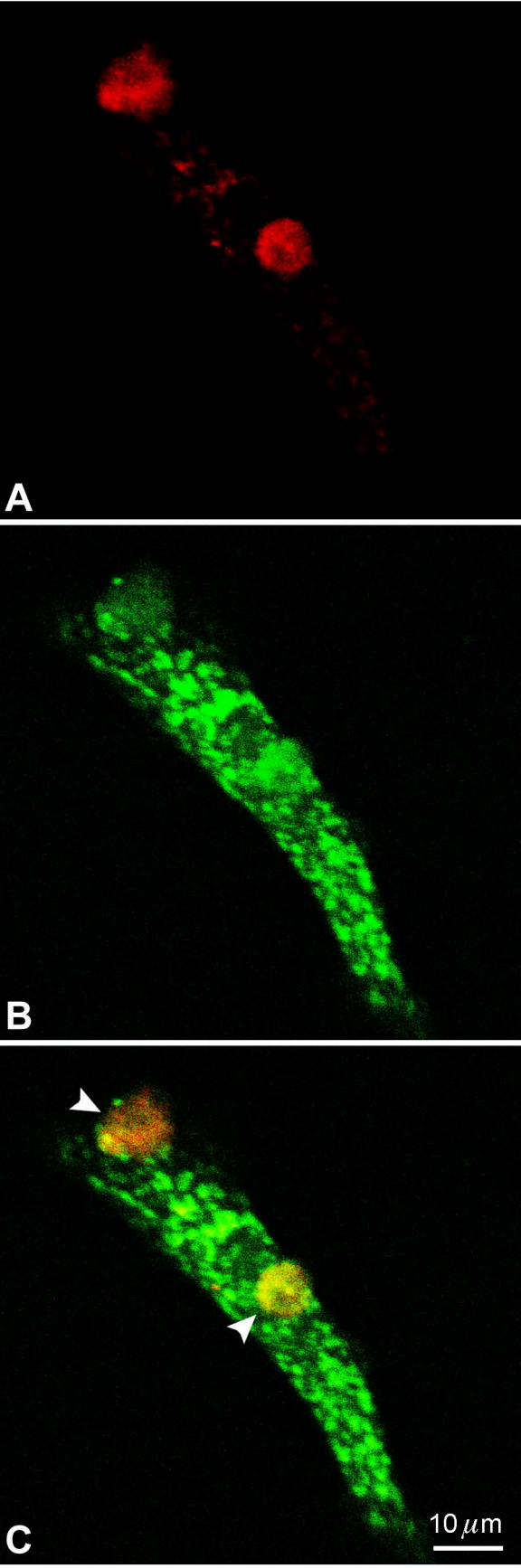
A
B
C
10 μm

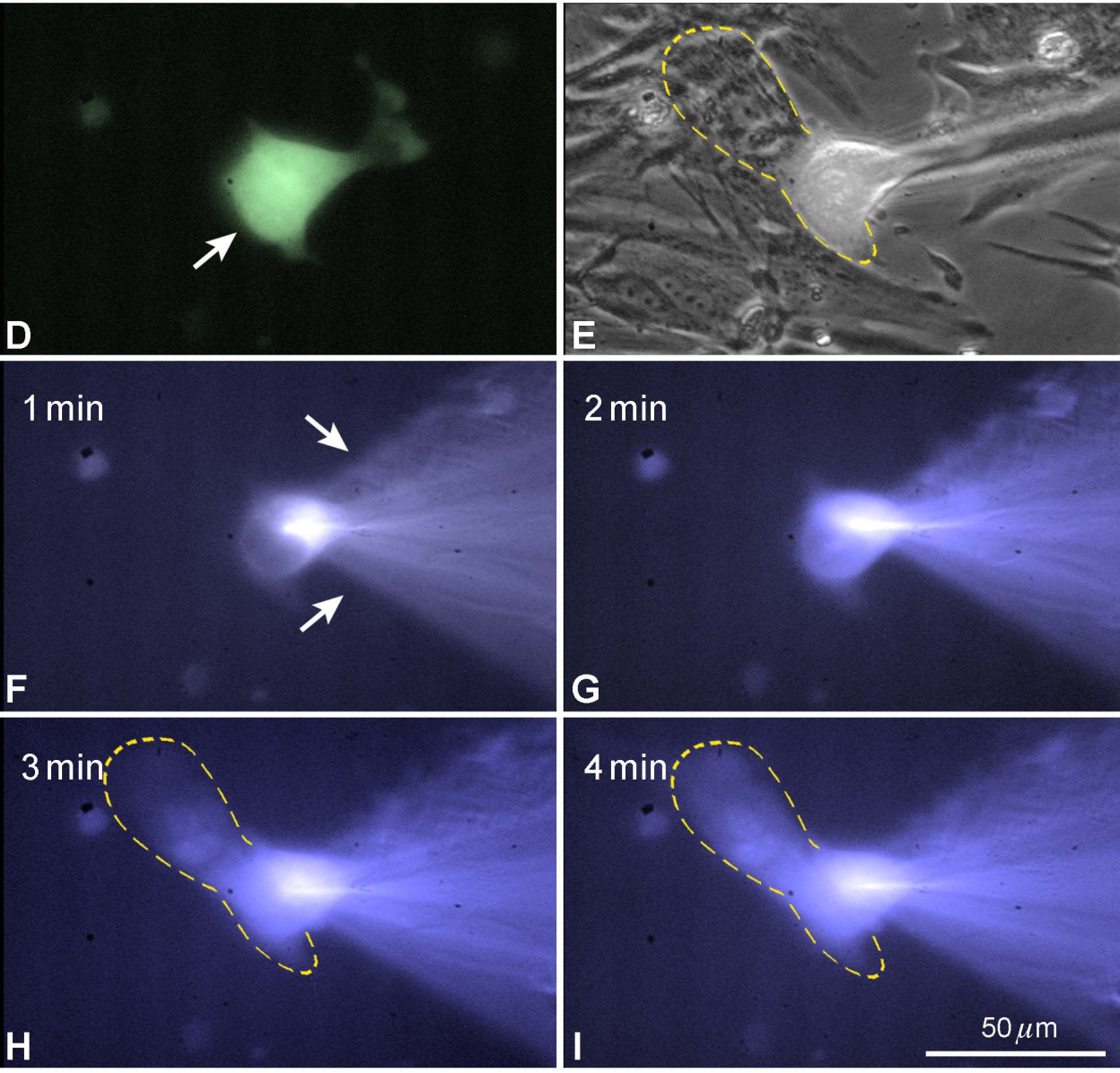
D
E
1 min
F
2 min
G
3 min
H
4 min
I
50 μm

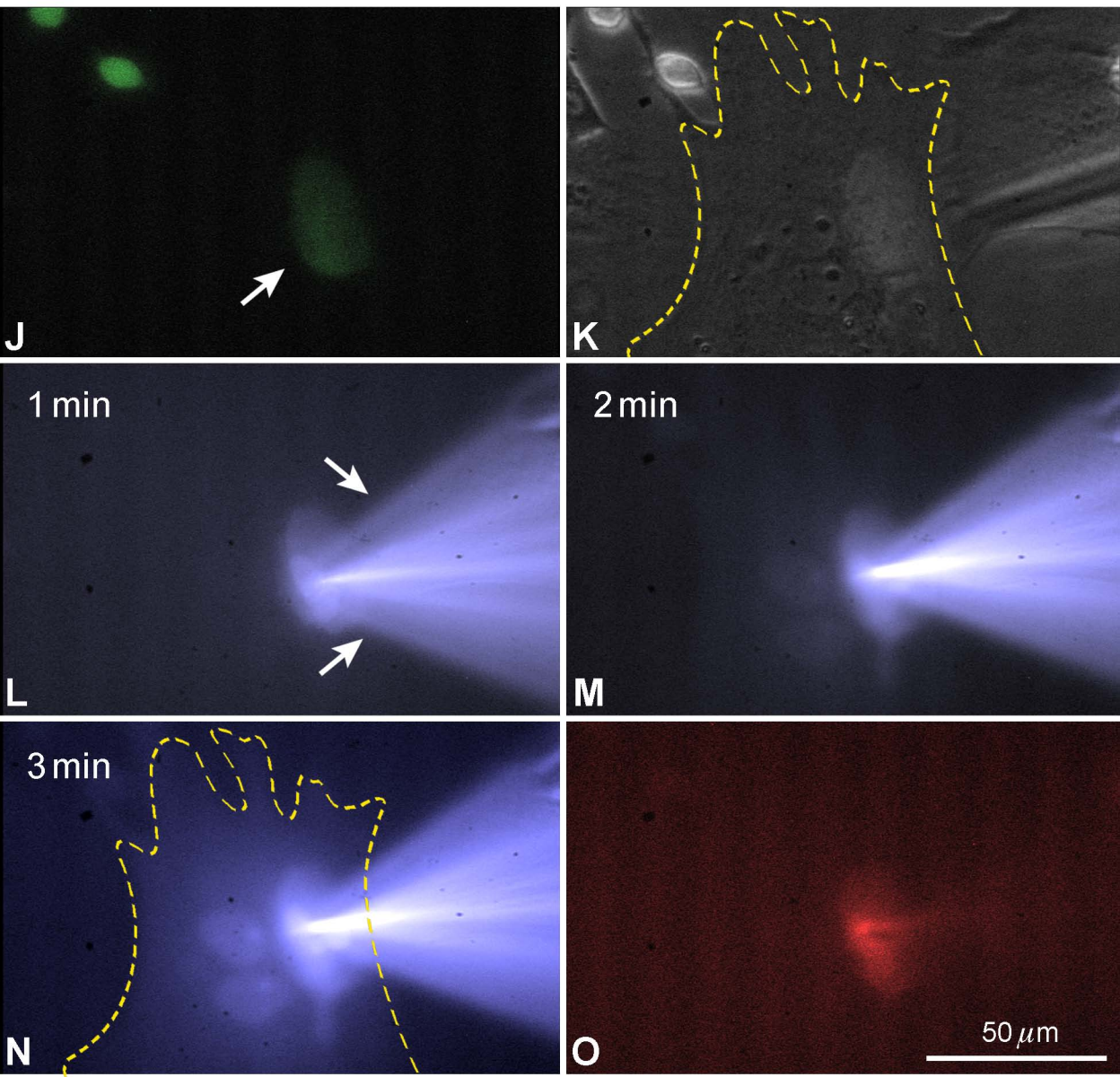
J
K
1 min
L
2 min
M
3 min
N
O
50 μm

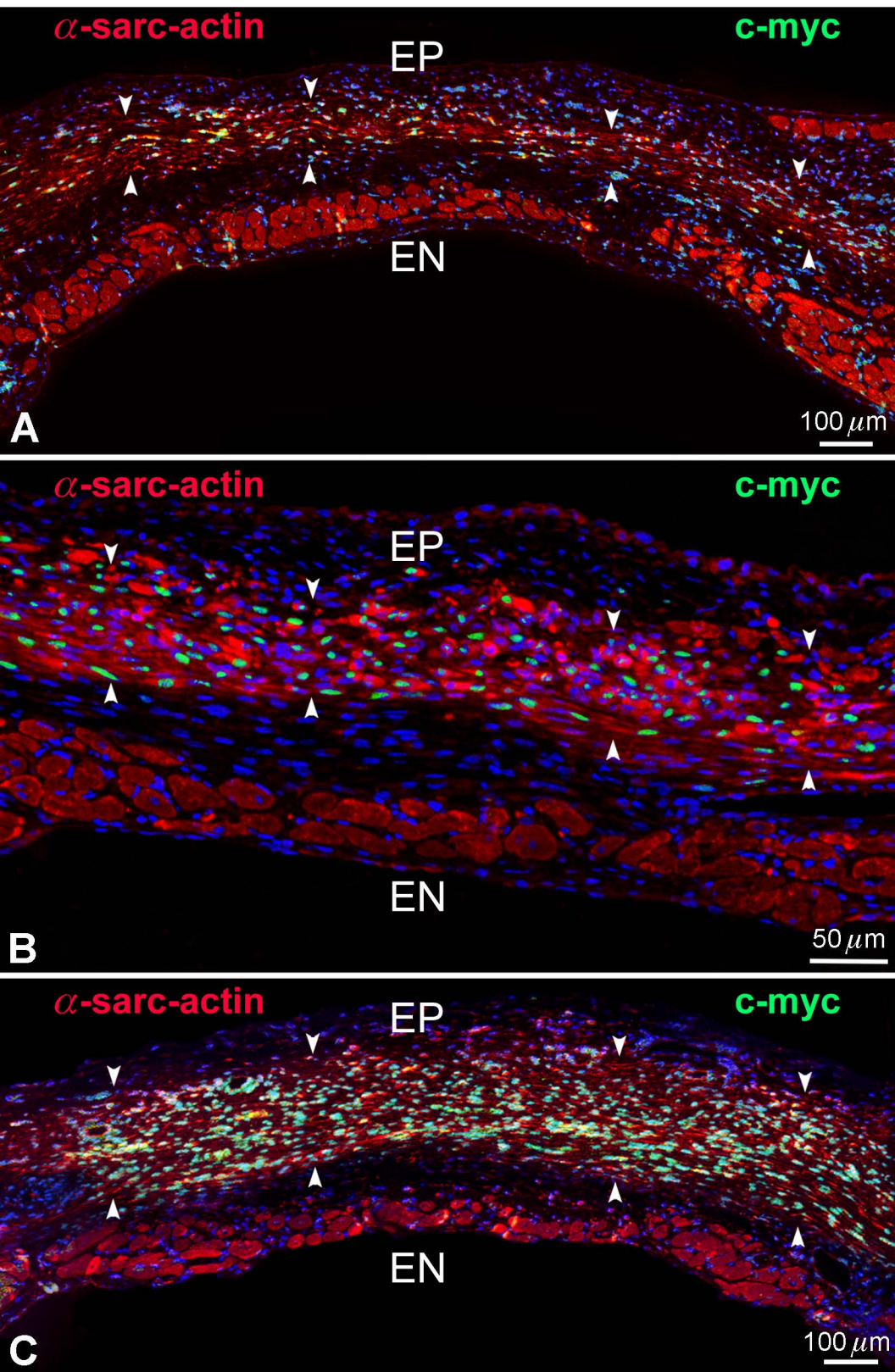
α-sarc-actin
c-myc
EP
EN
A
100 μm
α-sarc-actin
c-myc
EP
EN
B
50 μm
α-sarc-actin
c-myc
EP
EN
C
100 μm

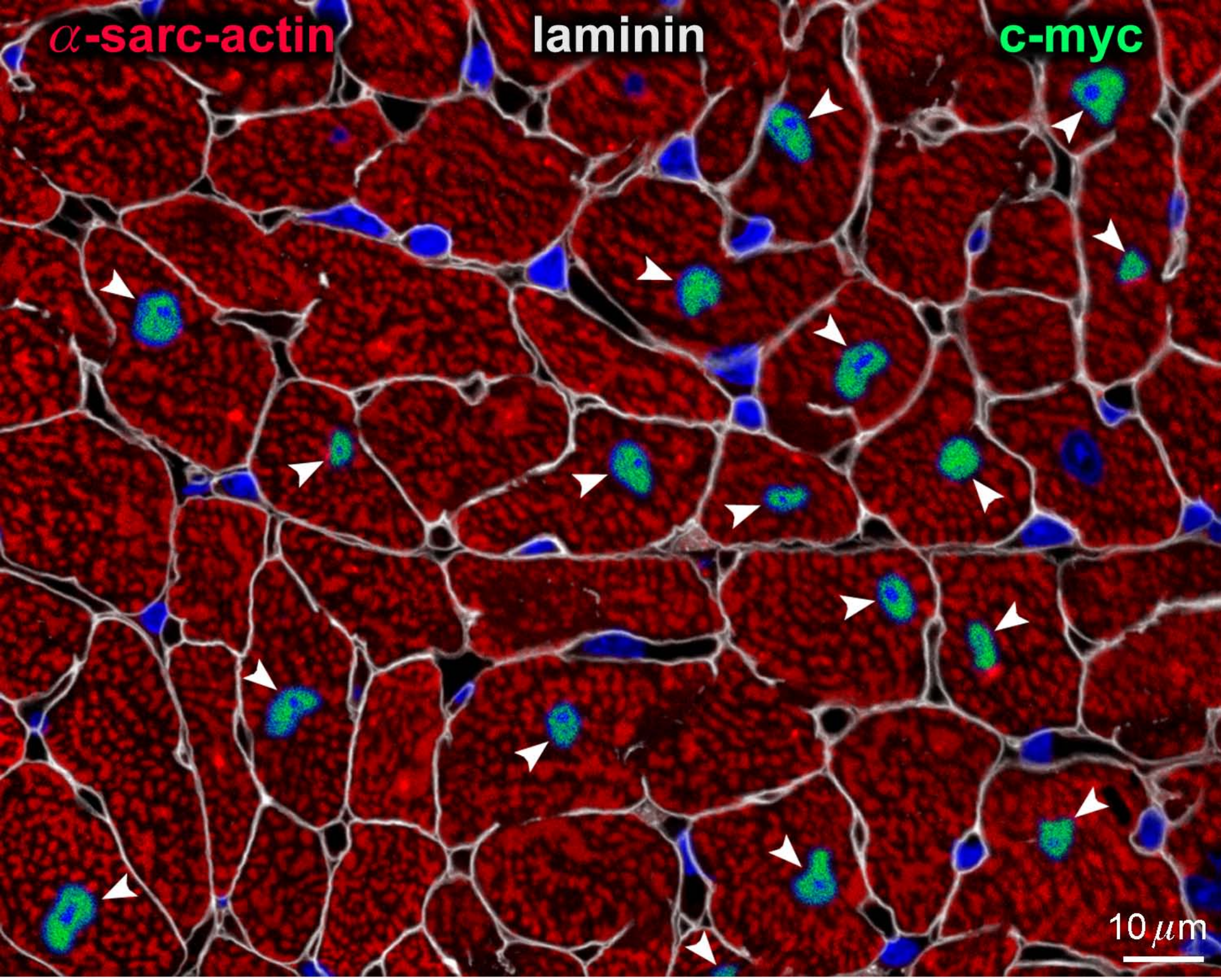
α-sarc-actin
laminin
c-myc
10 μm

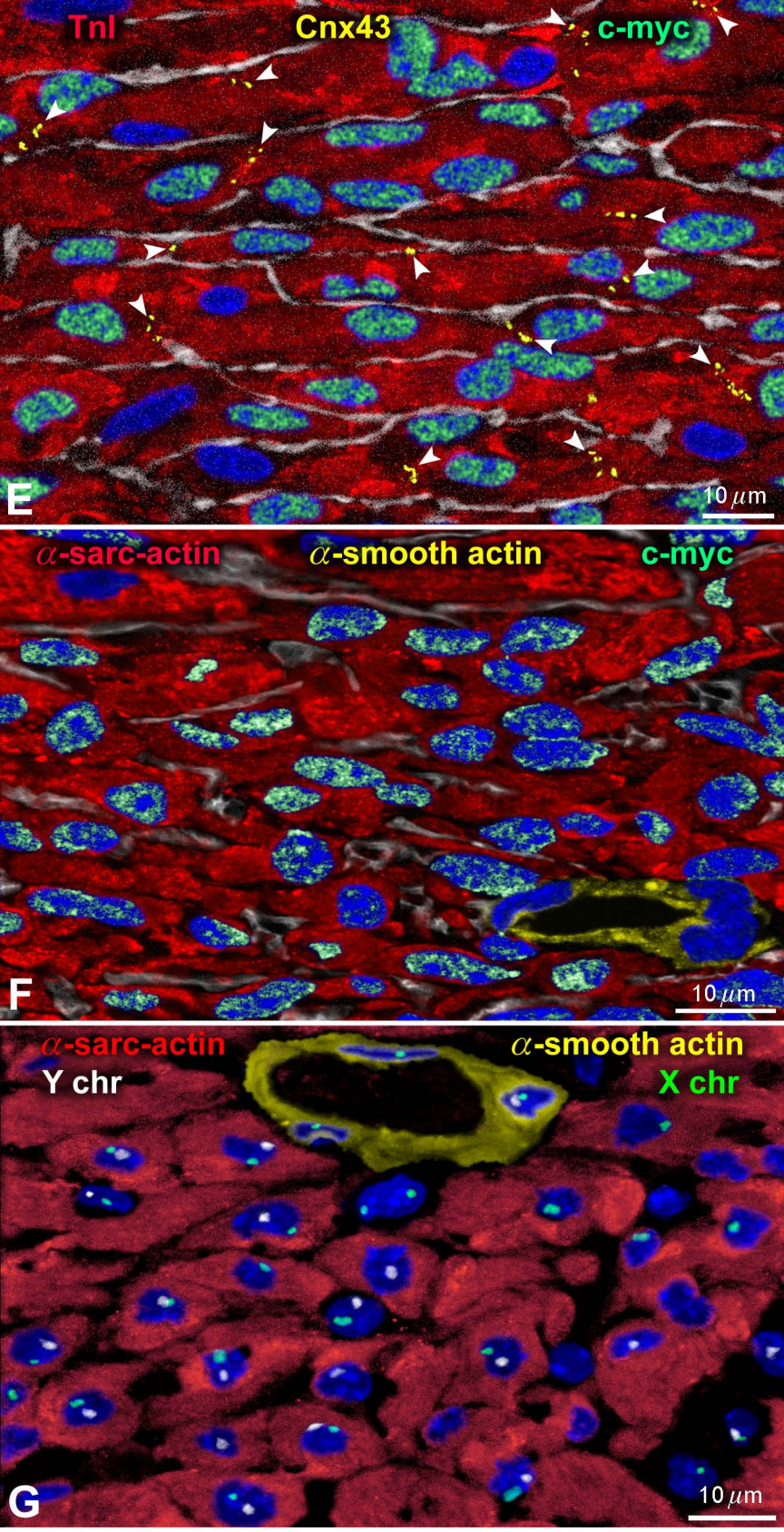
TnI
Cnx43
c-myc
E
10 μm
α-sarc-actin
α-smooth actin
c-myc
F
10 μm
α-sarc-actin
Y chr
α-smooth actin
X chr
G
10 μm

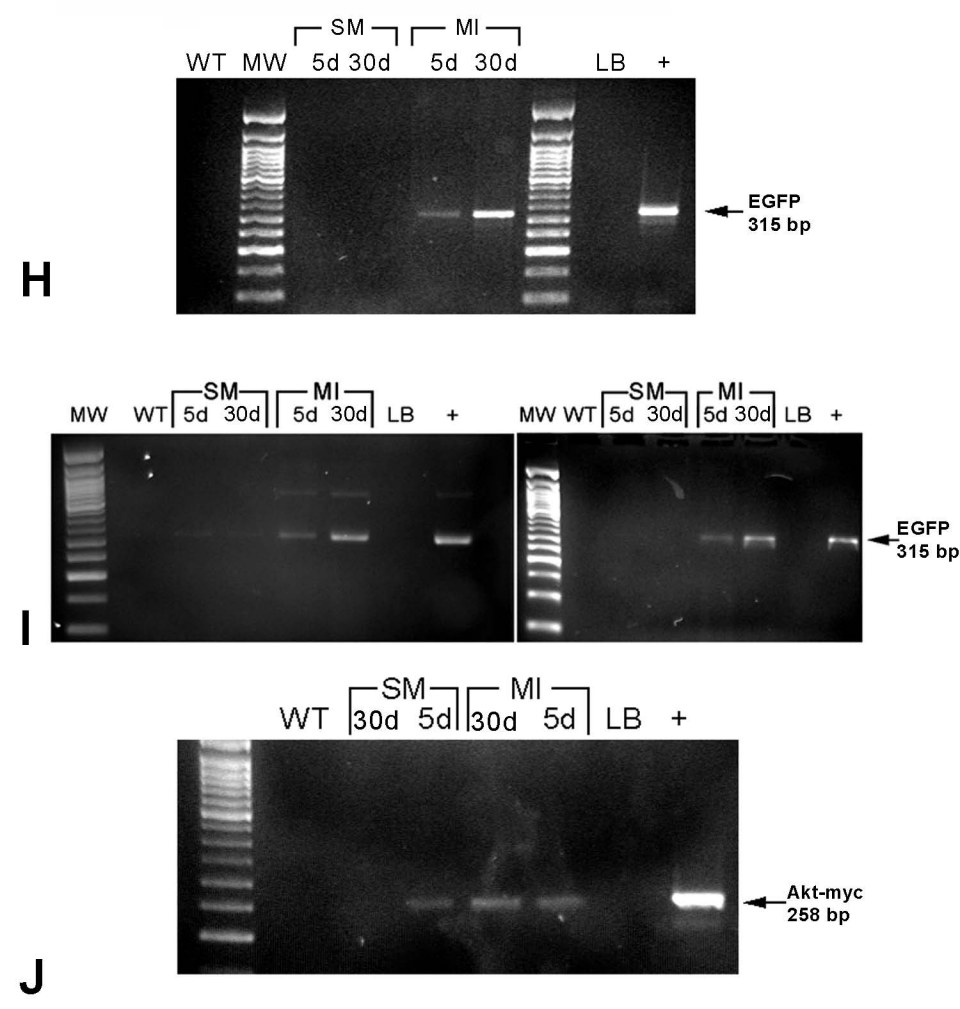
SM
MI
WT MW 5d 30d 5d 30d LB +
EGFP
315 bp
H
MW WT 5d 30d 5d 30d LB +
MW WT 5d 30d 5d 30d LB +
EGFP
315 bp
I
WT 30d 5d 30d 5d LB +
Akt-myc
258 bp
J

β-actin-EGFP (30 Days)

Sense

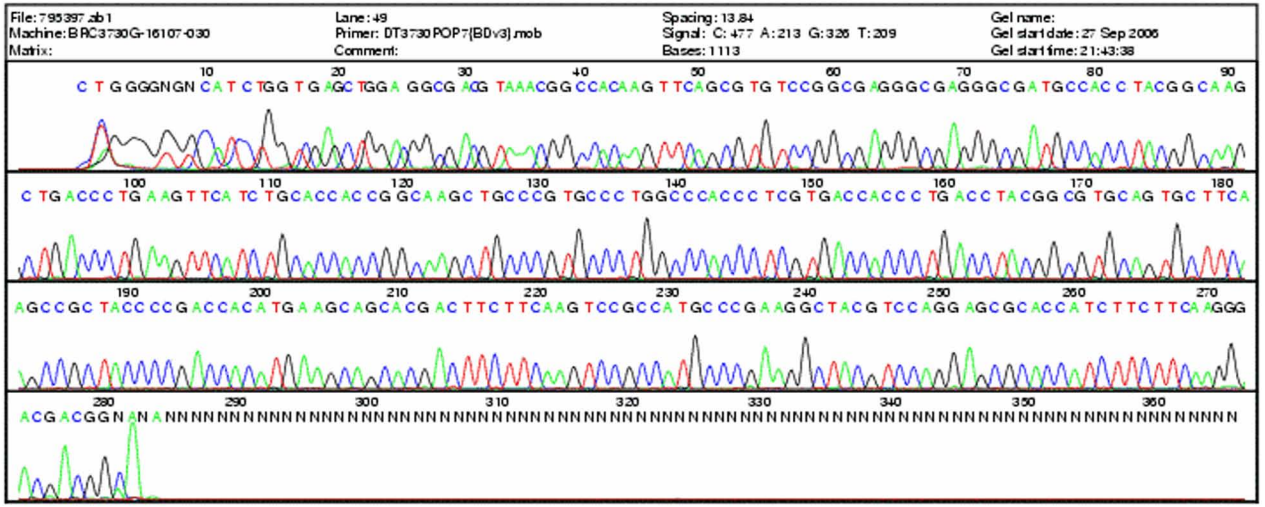

Antisense

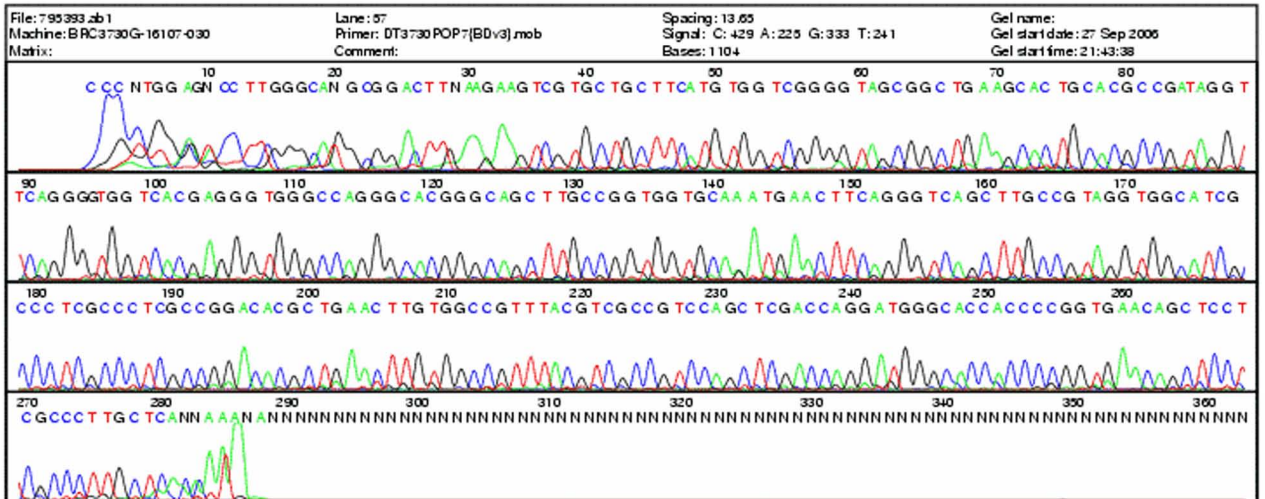

αMHC-EGFP (30 Days)

Sense

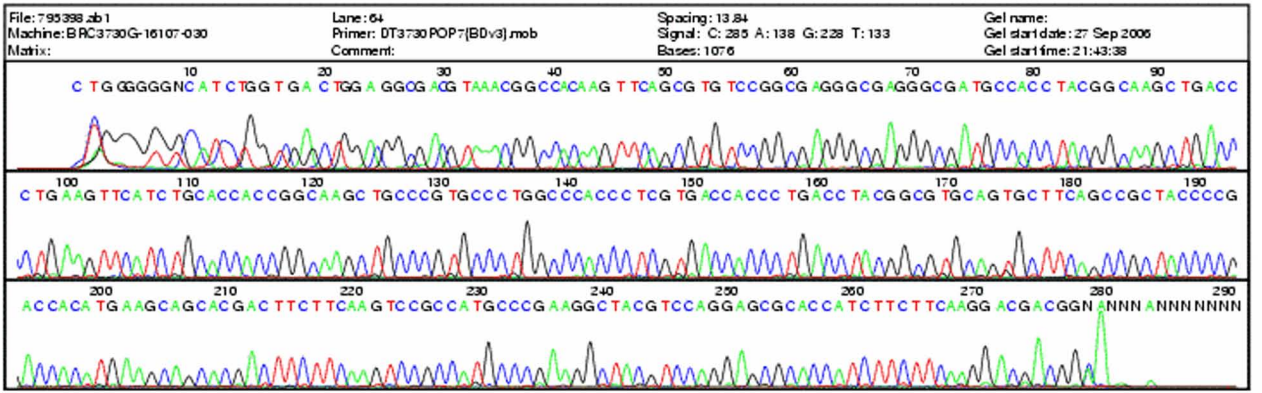

Antisense

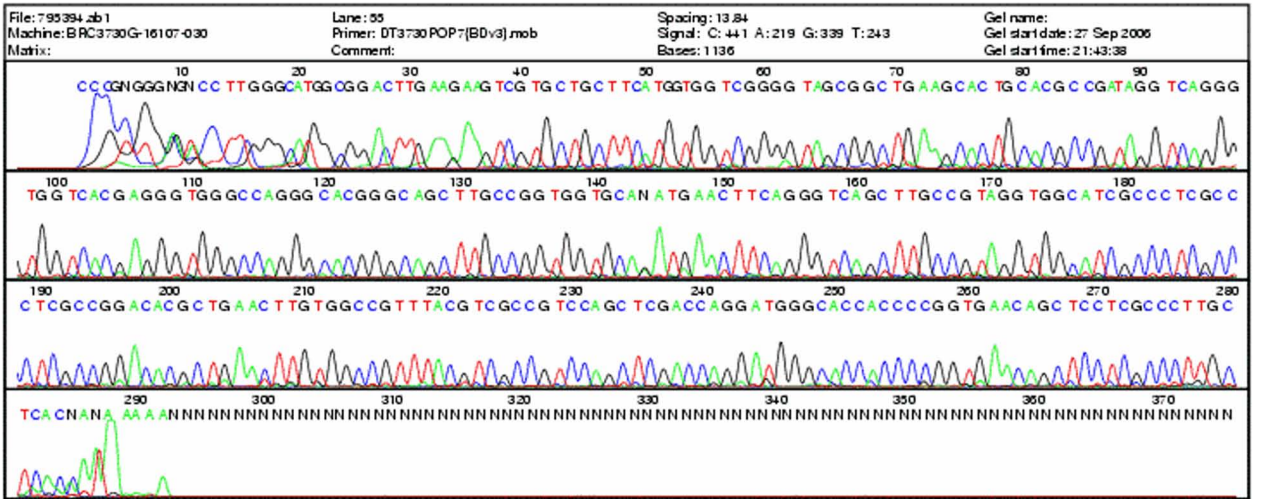

Akt-myc (30 Days)

Sense

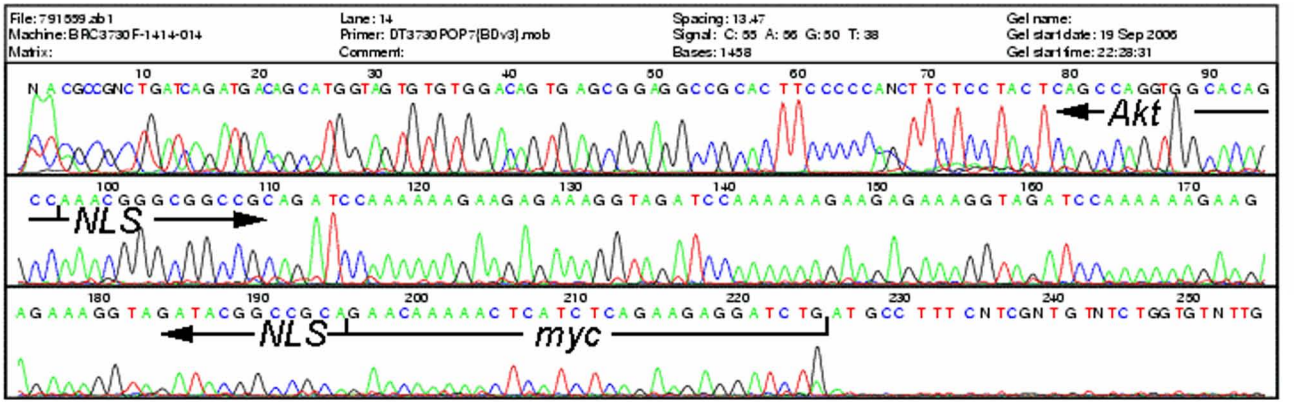

Antisense

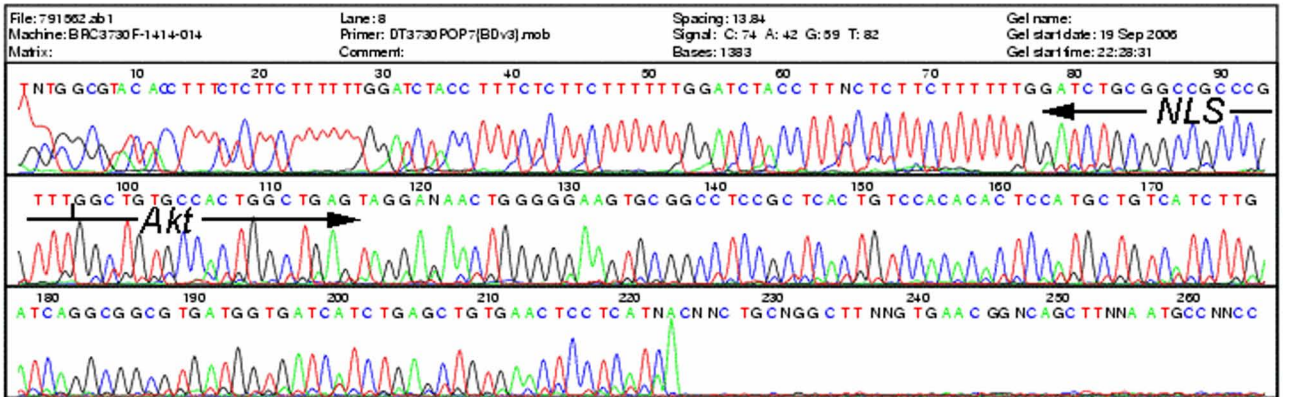

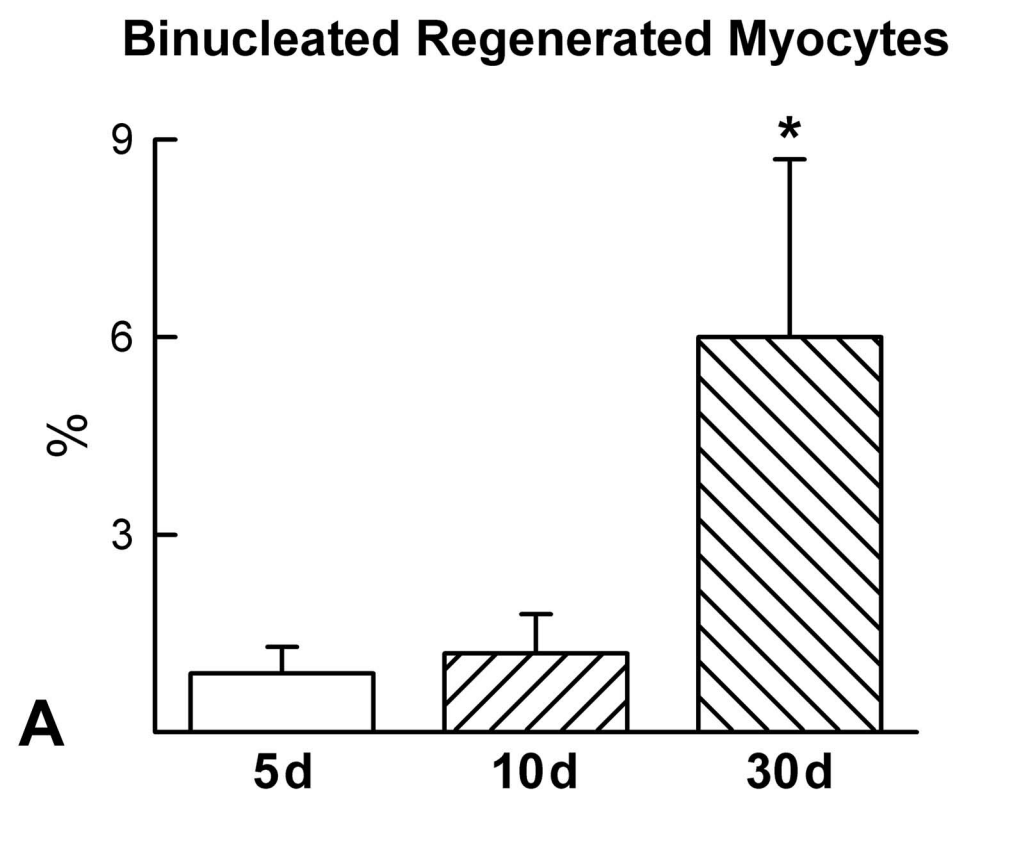
Binucleated Regenerated Myocytes
9
6
3
%
*
A
5d
10d
30d

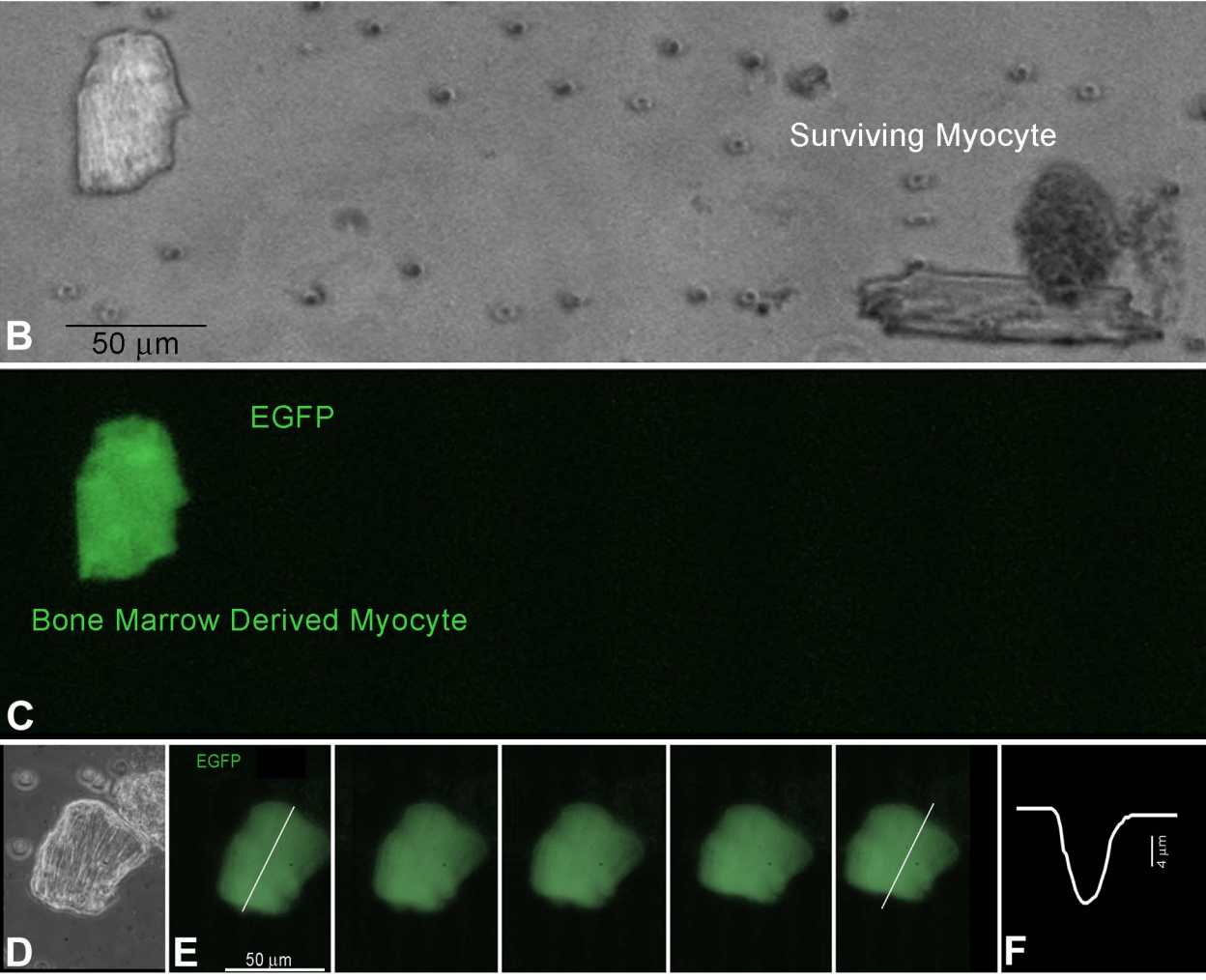
Surviving Myocyte
B
50 μm
EGFP
Bone Marrow Derived Myocyte
C
D
EGFP
E
50 μm
4 μm
F

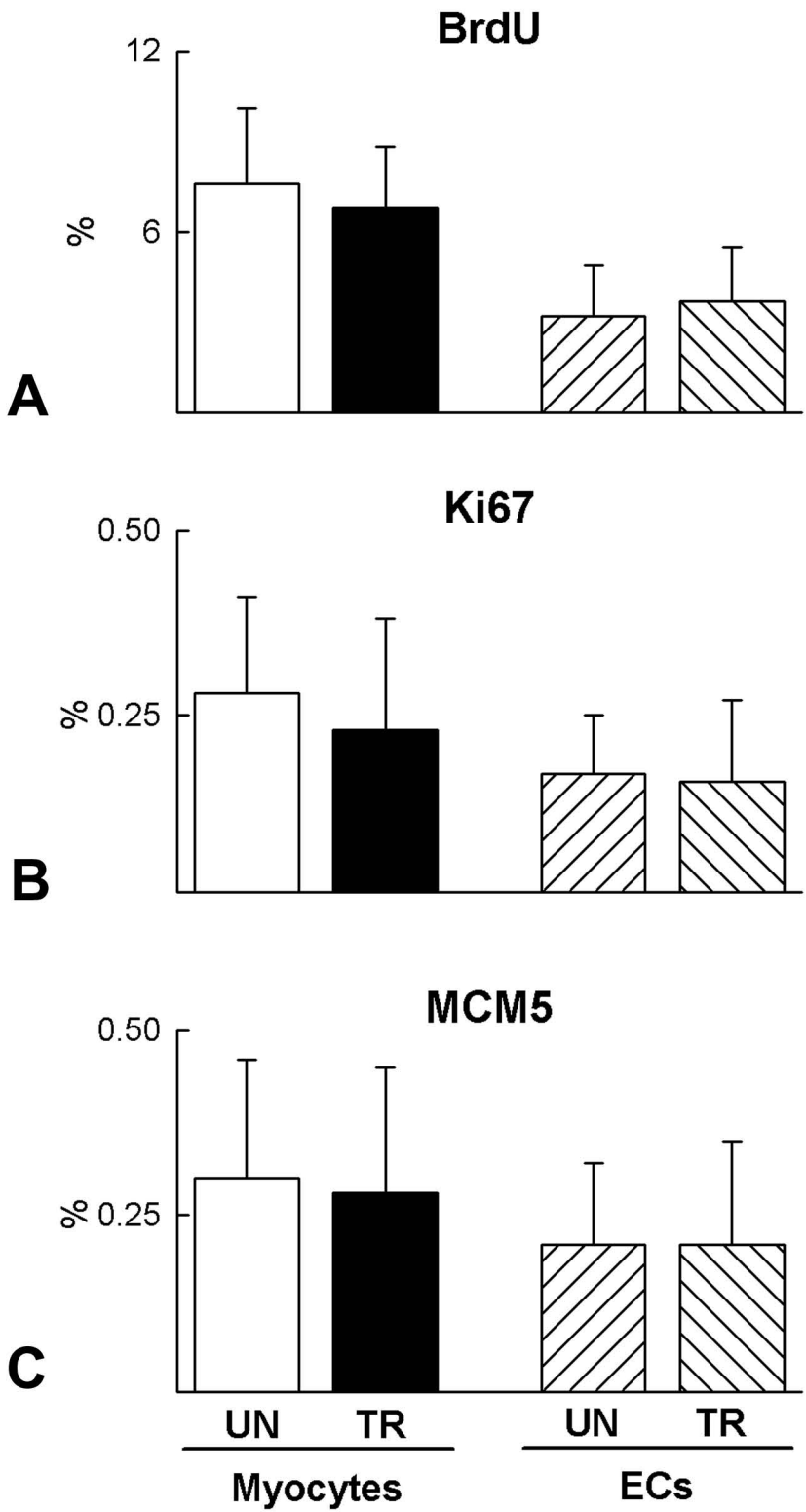
BrdU
12
%
6
A
Ki67
0.50
%
0.25
B
MCM5
0.50
%
0.25
C
UN
TR
UN
TR
Myocytes
ECs

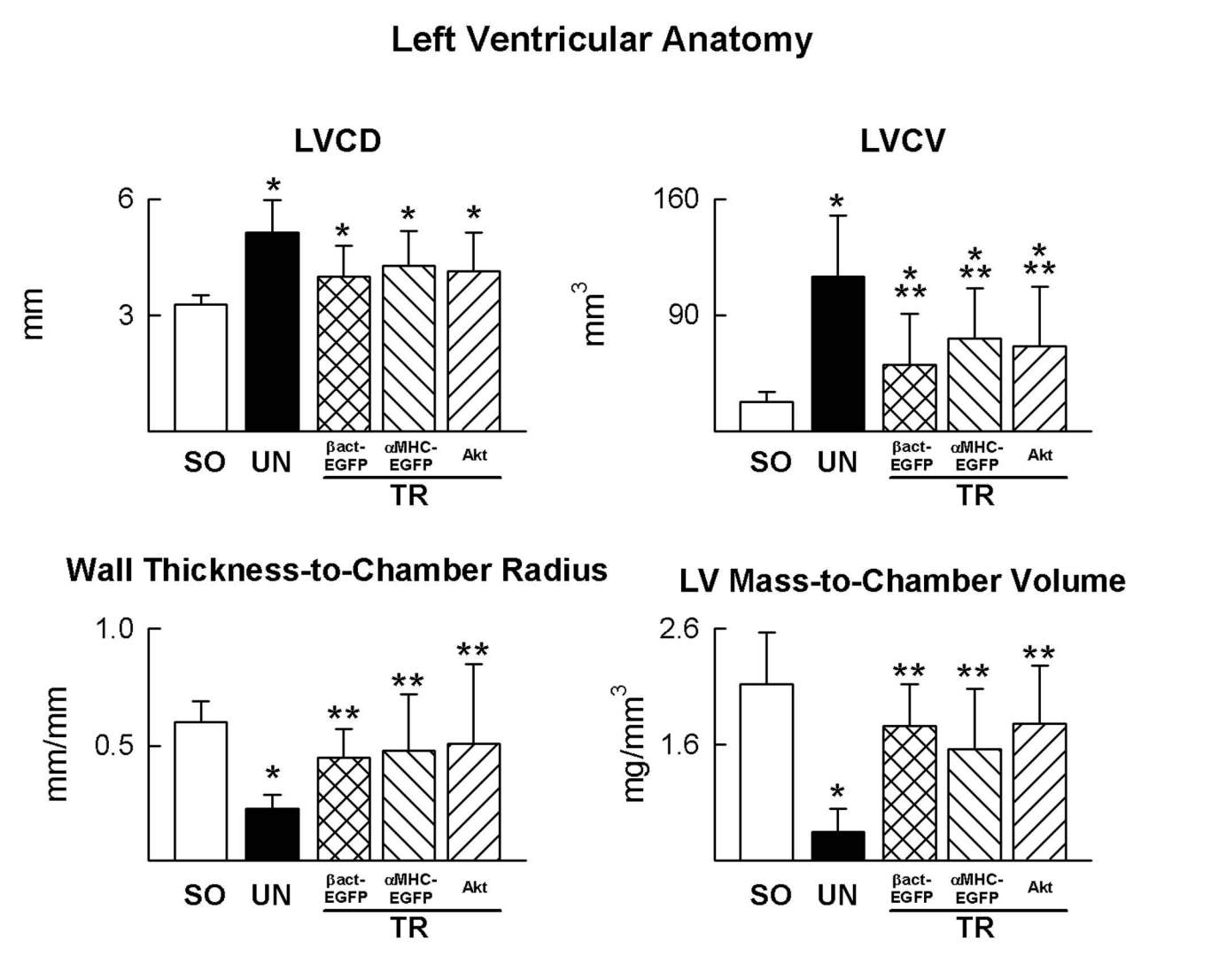
Left Ventricular Anatomy
LVCD
mm
6
3
SO
UN
βact-EGFP
αMHC-EGFP
Akt
TR
LVCV
mm3
160
90
Wall Thickness-to-Chamber Radius
mm/mm
1.0
0.5
LV Mass-to-Chamber Volume
mg/mm3
2.6
1.6

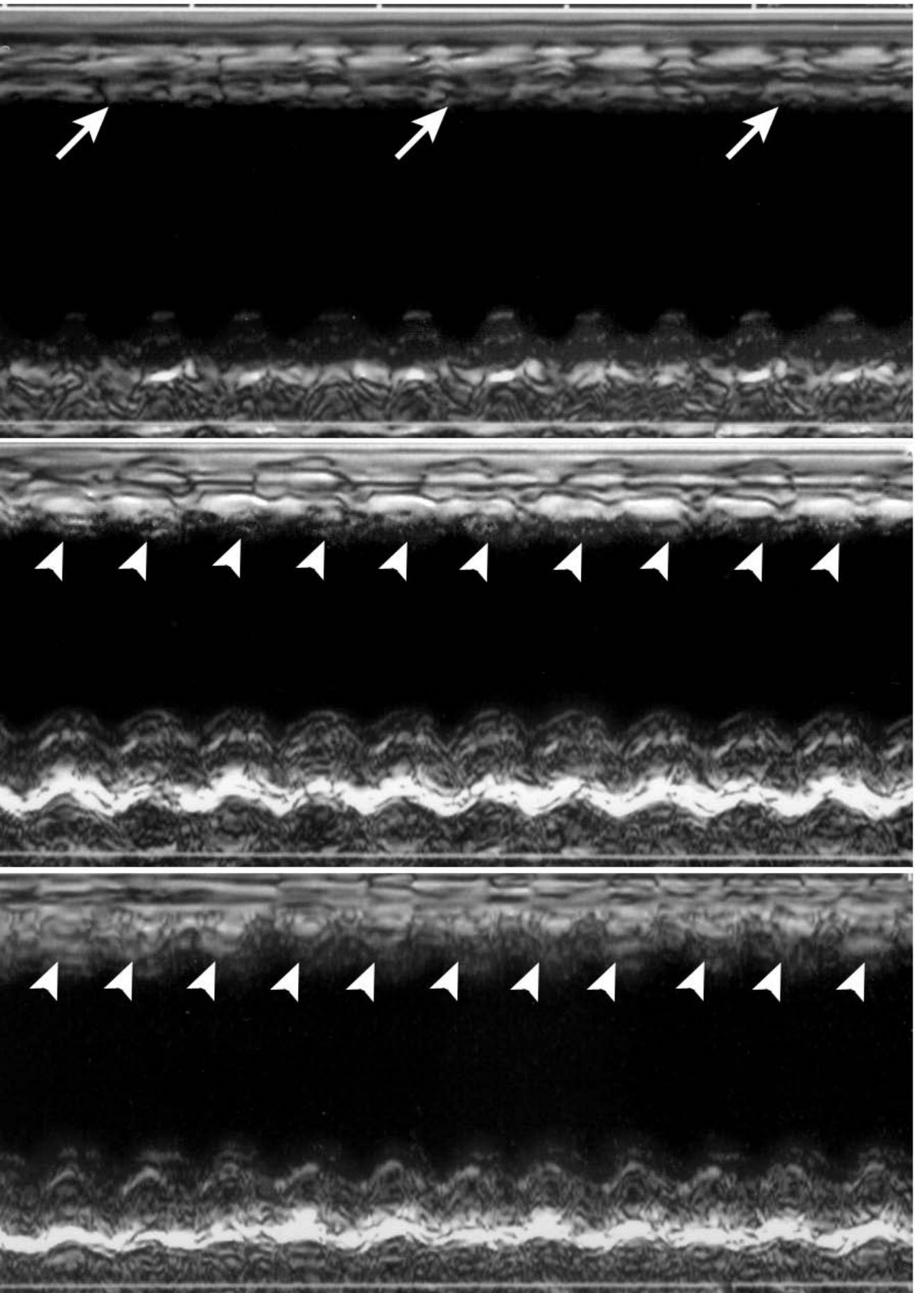

untreated

treated, 16d

treated, 30d

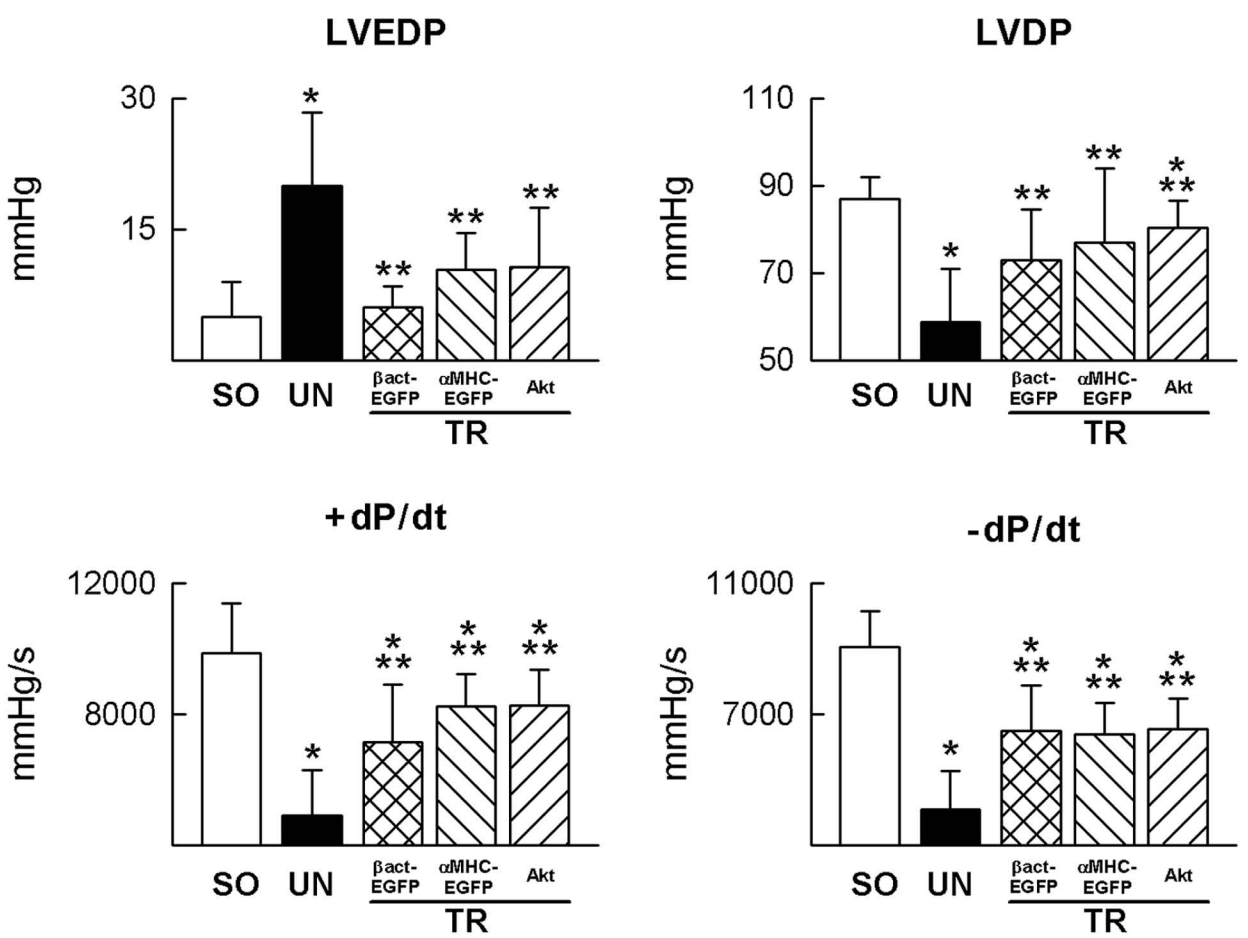
Left Ventricular Hemodynamics
LVEDP
mmHg
30
15
SO
UN
βact-EGFP
αMHC-EGFP
Akt
TR
LVDP
mmHg
110
90
70
50
+dP/dt
mmHg/s
12000
8000
-dP/dt
mmHg/s
11000
7000
F